

Principles of Radiation and Antennas

In Chapters 3, 4, 6, 7, 8, and 9, we studied the principles and applications of propagation and transmission of electromagnetic waves. The remaining important topic pertinent to electromagnetic wave phenomena is radiation of electromagnetic waves. We have, in fact, touched on the principle of radiation of electromagnetic waves in Chapter 3 when we derived the electromagnetic field due to the infinite plane sheet of time-varying, spatially uniform current density. We learned that the current sheet gives rise to uniform plane waves radiating away from the sheet to either side of it. We pointed out at that time that the infinite plane current sheet is, however, an idealized, hypothetical source. With the experience gained thus far in our study of the elements of engineering electromagnetics, we are now in a position to learn the principles of radiation from physical antennas, which is our goal in this chapter.

We begin the chapter with the derivation of the electromagnetic field due to an elemental wire antenna, known as the *Hertzian dipole*. After studying the radiation characteristics of the Hertzian dipole, we consider the example of a half-wave dipole to illustrate the use of superposition to represent an arbitrary wire antenna as a series of Hertzian dipoles to determine its radiation fields. We also discuss the principles of arrays of physical antennas and the concept of image antennas to take into account ground effects. Next we study radiation from aperture antennas. Finally, we consider briefly the receiving properties of antennas and learn of their reciprocity with the radiating properties.

10.1 HERTZIAN DIPOLE

The *Hertzian dipole* is an elemental antenna consisting of an infinitesimally long piece of wire carrying an alternating current $I(t)$, as shown in Fig. 10.1. To maintain the current flow in the wire, we postulate two point charges $Q_1(t)$ and

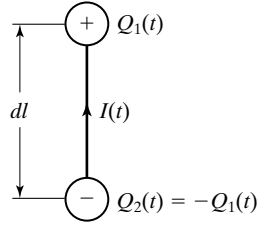


FIGURE 10.1
Hertzian dipole.

$Q_2(t)$ terminating the wire at its two ends, so that the law of conservation of charge is satisfied. Thus, if

$$I(t) = I_0 \cos \omega t \quad (10.1)$$

then

$$\frac{dQ_1}{dt} = I(t) = I_0 \cos \omega t \quad (10.2a)$$

$$\frac{dQ_2}{dt} = -I(t) = -I_0 \cos \omega t \quad (10.2b)$$

and

$$Q_1(t) = \frac{I_0}{\omega} \sin \omega t \quad (10.3a)$$

$$Q_2(t) = -\frac{I_0}{\omega} \sin \omega t = -Q_1(t) \quad (10.3b)$$

The time variations of I , Q_1 , and Q_2 , given by (10.1), (10.3a) and (10.3b), respectively, are illustrated by the curves and the series of sketches for the dipoles in Fig. 10.2, corresponding to one complete period. The different sizes of the arrows associated with the dipoles denote the different strengths of the current, whereas the number of the plus or minus signs indicates the strength of the charges.

To determine the electromagnetic field due to the Hertzian dipole, we consider the dipole to be situated at the origin and oriented along the z -axis, in a perfect dielectric medium. We shall use an approach based on the magnetic vector potential and obtain electric and magnetic fields consistent with Maxwell's equations, while fulfilling certain other pertinent requirements. We shall begin with the magnetic vector potential for the static case and then extend it to the time-varying current element. To do this, we recall from Section 5.2 that for a current element of length $d\mathbf{l} = dl \mathbf{a}_z$ situated at the origin, as shown in Fig. 10.3 and carrying current I , the magnetic field at a point $P(r, \theta, \phi)$ is given by

$$\mathbf{A} = \frac{\mu I d\mathbf{l}}{4\pi r} = \frac{\mu I dl}{4\pi r} \mathbf{a}_z \quad (10.4)$$

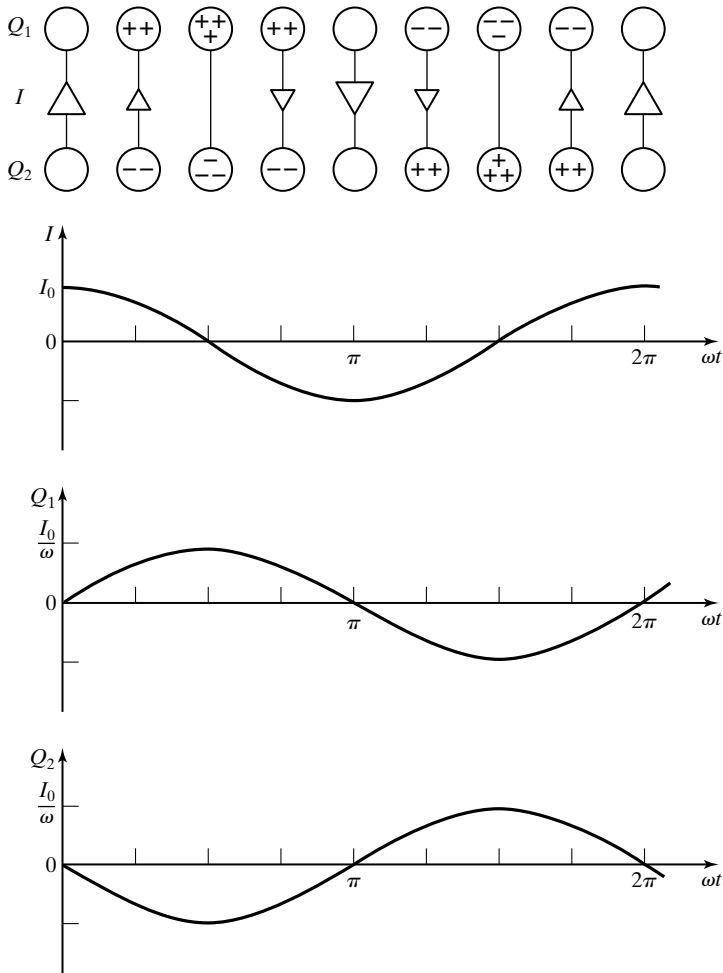


FIGURE 10.2

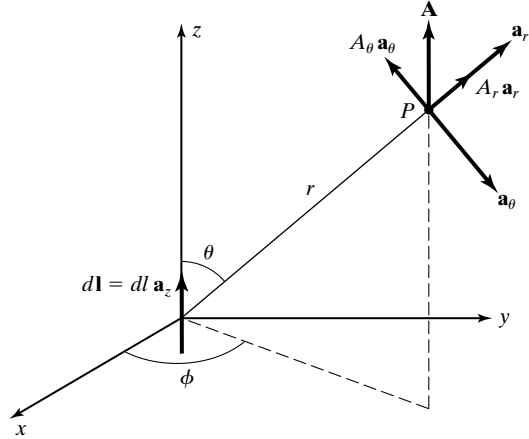
Time variations of charges and current associated with the Hertzian dipole.

If the current in the element is now assumed to be time varying in the manner $I = I_0 \cos \omega t$, we might expect the corresponding magnetic vector potential to be that in (10.4) with I replaced by $I_0 \cos \omega t$. Proceeding in this manner would however lead to fields inconsistent with Maxwell's equations. The reason is that time-varying electric and magnetic fields give rise to wave propagation, according to which the effect of the source current at a given value of time is felt at a distance r from the origin after a time delay of r/v_p , where v_p is the velocity of propagation of the wave. Conversely, the effect felt at a distance r from the origin at time t is due to the current that existed at the origin at an earlier time $(t - r/v_p)$. Thus, for the time-varying

Retarded potential

FIGURE 10.3

For finding the magnetic vector potential due to an infinitesimal current element.



current element $I_0 dl \cos \omega t \mathbf{a}_z$ situated at the origin, the magnetic vector potential is given by

$$\begin{aligned} \mathbf{A} &= \frac{\mu I_0 dl}{4\pi r} \cos \omega \left(t - \frac{r}{v_p} \right) \mathbf{a}_z \\ &= \frac{\mu I_0 dl}{4\pi r} \cos (\omega t - \beta r) \mathbf{a}_z \end{aligned} \quad (10.5)$$

where we have replaced ω/v_p by β , the phase constant. The result given by (10.5) is known as the *retarded* magnetic vector potential in view of the phase-lag factor βr contained in it.

To augment the reasoning behind the retarded magnetic vector potential, recall that in Section 5.1, we derived differential equations for the electromagnetic potentials. For the magnetic vector potential, we obtained

$$\nabla^2 \mathbf{A} - \mu\epsilon \frac{\partial^2 \mathbf{A}}{\partial t^2} = -\mu \mathbf{J} \quad (10.6)$$

which reduces to

$$\nabla^2 A_z - \mu\epsilon \frac{\partial^2 A_z}{\partial t^2} = -\mu J_z \quad (10.7)$$

for $\mathbf{A} = A_z \mathbf{a}_z$ and $\mathbf{J} = J_z \mathbf{a}_z$. Equation (10.7) has the form of the wave equation, except in three dimensions and with the source term on the right side. Thus, the solution for A_z must be of the form of a traveling wave while reducing to the static field case for no time variations.

Expressing \mathbf{A} in (10.5) in terms of its components in spherical coordinates, as shown in Fig. 10.3, we obtain

$$\mathbf{A} = \frac{\mu I_0 dl \cos(\omega t - \beta r)}{4\pi r} (\cos \theta \mathbf{a}_r - \sin \theta \mathbf{a}_\theta) \quad (10.8)$$

Fields due to Hertzian dipole

The magnetic field due to the Hertzian dipole is then given by

$$\begin{aligned} \mathbf{H} &= \frac{\mathbf{B}}{\mu} = \frac{1}{\mu} \nabla \times \mathbf{A} \\ &= \frac{1}{\mu} \begin{vmatrix} \mathbf{a}_r & \mathbf{a}_\theta & \mathbf{a}_\phi \\ r^2 \sin \theta & r \sin \theta & r \\ \frac{\partial}{\partial r} & \frac{\partial}{\partial \theta} & \frac{\partial}{\partial \phi} \end{vmatrix} = \frac{1}{\mu r} \left[\frac{\partial}{\partial r} (r A_\theta) - \frac{\partial A_r}{\partial \theta} \right] \mathbf{a}_\phi \end{aligned}$$

or

$$\mathbf{H} = \frac{I_0 dl \sin \theta}{4\pi} \left[\frac{\cos(\omega t - \beta r)}{r^2} - \frac{\beta \sin(\omega t - \beta r)}{r} \right] \mathbf{a}_\phi \quad (10.9)$$

Using Maxwell's curl equation for \mathbf{H} with \mathbf{J} set equal to zero in view of perfect dielectric medium, we then have

$$\begin{aligned} \frac{\partial \mathbf{E}}{\partial t} &= \frac{1}{\epsilon} \nabla \times \mathbf{H} \\ &= \frac{1}{\epsilon} \begin{vmatrix} \mathbf{a}_r & \mathbf{a}_\theta & \mathbf{a}_\phi \\ r^2 \sin \theta & r \sin \theta & r \\ \frac{\partial}{\partial r} & \frac{\partial}{\partial \theta} & \frac{\partial}{\partial \phi} \end{vmatrix} \\ &= \frac{1}{\epsilon r^2 \sin \theta} \frac{\partial}{\partial \theta} (r \sin \theta H_\phi) \mathbf{a}_r - \frac{1}{\epsilon r \sin \theta} \frac{\partial}{\partial r} (r \sin \theta H_\phi) \mathbf{a}_\theta \end{aligned}$$

or

$$\begin{aligned} \mathbf{E} &= \frac{2I_0 dl \cos \theta}{4\pi \epsilon \omega} \left[\frac{\sin(\omega t - \beta r)}{r^3} + \frac{\beta \cos(\omega t - \beta r)}{r^2} \right] \mathbf{a}_r \\ &+ \frac{I_0 dl \sin \theta}{4\pi \epsilon \omega} \left[\frac{\sin(\omega t - \beta r)}{r^3} + \frac{\beta \cos(\omega t - \beta r)}{r^2} \right. \\ &\left. - \frac{\beta^2 \sin(\omega t - \beta r)}{r} \right] \mathbf{a}_\theta \end{aligned} \quad (10.10)$$

Equations (10.10) and (10.9) represent the electric and magnetic fields, respectively, due to the Hertzian dipole. The following observations are pertinent to these field expressions:

1. They satisfy the two Maxwell's curl equations. In fact, we have obtained (10.10) from (10.9) by using the curl equation for \mathbf{H} . The reader is urged to verify that (10.9) follows from (10.10) through the curl equation for \mathbf{E} .
2. They contain terms involving $1/r^3$, $1/r^2$, and $1/r$. Far from the dipole such that $\beta r \gg 1$, the $1/r^3$ and $1/r^2$ terms are negligible compared to the $1/r$ terms so that the fields vary inversely with r . Furthermore, for any value of r , the time-average value of the θ -component of the Poynting vector due to the fields is zero, and the contribution to the time-average value of the r -component is completely from the $1/r$ terms (see Problem P10.2). Thus, the time-average Poynting vector varies proportionately to $1/r^2$ and is directed entirely in the radial direction. This is consistent with the physical requirement that for the time-average power crossing all possible spherical surfaces centered at the dipole to be the same, the power density must be inversely proportional to r^2 , since the surface areas of the spherical surfaces are proportional to the squares of their radii.
3. For $\beta r \ll 1$, the $1/r^3$ terms dominate the $1/r^2$ terms which in turn dominate the $1/r$ terms. Also, $\sin(\omega t - \beta r) \approx (\sin \omega t - \beta r \cos \omega t)$ and $\cos(\omega t - \beta r) \approx (\cos \omega t + \beta r \sin \omega t)$, so that

$$\mathbf{E} \approx \frac{I_0 dl \sin \omega t}{4\pi\epsilon_0 r^3} (2 \cos \theta \mathbf{a}_r + \sin \theta \mathbf{a}_\theta) \quad (10.11)$$

$$\mathbf{H} \approx \frac{I_0 dl \cos \omega t}{4\pi r^2} \sin \theta \mathbf{a}_\phi \quad (10.12)$$

Equation (10.11) is the same as (5.37) with Q replaced by $(I_0/\omega) \sin \omega t$, that is, $Q_1(t)$ in Fig. 10.1, and d replaced by dl . Equation (10.12) gives the same \mathbf{B} as the magnetic field given by Biot–Savart law applied to a current element $I dl \mathbf{a}_z$ at the origin and then I replaced by $I_0 \cos \omega t$, that is, $I(t)$ in Fig. 10.1. Thus, electrically close to the dipole, where retardation effects are negligible, the field expressions approach toward the corresponding static field expressions with the static source terms simply replaced by the time-varying source terms.

Example 10.1 Electric and magnetic fields of a Hertzian dipole

Let us consider in free space a Hertzian dipole of length 0.1 m situated at the origin and along the z -axis, carrying the current $10 \cos 2\pi \times 10^7 t$ A. We wish to obtain the electric and magnetic fields at the point $(5, \pi/6, 0)$.

For convenience in computation of the amplitudes and phase angles of the field components, we shall express the field components in phasor form. Thus, replacing $\cos(\omega t - \beta r)$ by $e^{-j\beta r}$ and $\sin(\omega t - \beta r)$ by $-je^{-j\beta r}$, we have

$$\begin{aligned}\bar{E}_r &= \frac{2I_0 dl \cos \theta}{4\pi\epsilon\omega} \left(-\frac{j}{r^3} + \frac{\beta}{r^2} \right) e^{-j\beta r} \\ &= \frac{2\beta^2\eta I_0 dl \cos \theta}{4\pi} \left[-j\frac{1}{(\beta r)^3} + \frac{1}{(\beta r)^2} \right] e^{-j\beta r}\end{aligned}\quad (10.13)$$

$$\begin{aligned}\bar{E}_\theta &= \frac{I_0 dl \sin \theta}{4\pi\epsilon\omega} \left(-\frac{j}{r^3} + \frac{\beta}{r^2} + \frac{j\beta^2}{r} \right) e^{-j\beta r} \\ &= \frac{\beta^2\eta I_0 dl \sin \theta}{4\pi} \left[-j\frac{1}{(\beta r)^3} + \frac{1}{(\beta r)^2} + j\frac{1}{\beta r} \right] e^{-j\beta r}\end{aligned}\quad (10.14)$$

$$\begin{aligned}\bar{H}_\phi &= \frac{I_0 dl \sin \theta}{4\pi} \left(\frac{1}{r^2} + \frac{j\beta}{r} \right) e^{-j\beta r} \\ &= \frac{\beta^2 I_0 dl \sin \theta}{4\pi} \left[\frac{1}{(\beta r)^2} + j\frac{1}{\beta r} \right] e^{-j\beta r}\end{aligned}\quad (10.15)$$

where $\eta = \sqrt{\mu/\epsilon}$ is the intrinsic impedance of the medium. Using $I_0 = 10$ A, $dl = 0.1$ m, $f = 10^7$ Hz, $\mu = \mu_0$, $\epsilon = \epsilon_0$, $\beta = \pi/15$, $\eta = 120\pi$, $r = 5$ m, and $\theta = \pi/6$, and carrying out the computations, we obtain

$$\begin{aligned}\bar{E}_r &= 2.8739 \angle -103.679^\circ \text{ V/m} \\ \bar{E}_\theta &= 0.6025 \angle -54.728^\circ \text{ V/m} \\ \bar{H}_\phi &= 0.0023 \angle -13.679^\circ \text{ A/m}\end{aligned}$$

Thus, the required fields are

$$\begin{aligned}\mathbf{E} &= 2.8739 \cos(2\pi \times 10^7 t - 0.576\pi) \mathbf{a}_r \\ &\quad + 0.6025 \cos(2\pi \times 10^7 t - 0.304\pi) \mathbf{a}_\theta \text{ V/m} \\ \mathbf{H} &= 0.0023 \cos(2\pi \times 10^7 t - 0.076\pi) \mathbf{a}_\phi \text{ A/m}\end{aligned}$$

K10.1. Hertzian dipole; Retarded magnetic vector potential; Complete electromagnetic field; Behavior far from the dipole ($\beta r \gg 1$); Behavior close to the dipole ($\beta r \ll 1$).

D10.1. Consider a Hertzian dipole of length 0.1λ carrying sinusoidally time-varying current of amplitude 4π A. Find the magnitude of the electric dipole moment for each of the following cases: **(a)** $f = 10$ MHz, medium is free space; **(b)** $f = 100$ kHz, medium is free space; and **(c)** $f = 25$ kHz, medium is seawater ($\sigma = 4$ S/m, $\epsilon = 80\epsilon_0$, and $\mu = \mu_0$).

Ans. **(a)** 6×10^{-7} C-m; **(b)** 6×10^{-3} C-m; **(c)** 8×10^{-5} C-m.

D10.2. Three Hertzian dipoles of lengths 1, 1, and 2 m are situated at the origin oriented along the positive x -, y -, and z -axes, respectively, and carrying currents $1 \cos 2\pi \times 10^6 t$, $2 \sin 2\pi \times 10^6 t$, and $2 \cos 2\pi \times 10^6 t$ A, respectively. The medium is free space. Find the following at $(0, 0, 50)$ in Cartesian coordinates: **(a)** E_x ; **(b)** E_y ; and **(c)** E_z .

Ans. **(a)** $12.051 \cos(2\pi \times 10^6 t + 0.696\pi)$ mV/m; **(b)** $24.102 \cos(2\pi \times 10^6 t + 0.196\pi)$ mV/m; **(c)** $0.1327 \cos(2\pi \times 10^6 t - 0.576\pi)$ V/m.

10.2 RADIATION RESISTANCE AND DIRECTIVITY

Radiation fields

In the preceding section, we derived the expressions for the complete electromagnetic field due to the Hertzian dipole. These expressions look very complicated. Fortunately, it is seldom necessary to work with the complete field expressions because one is often interested in the field far from the dipole that is governed predominantly by the terms involving $1/r$. Thus, from (10.10) and (10.9), we find that for a Hertzian dipole of length dl oriented along the z -axis and carrying current

$$I = I_0 \cos \omega t \quad (10.16a)$$

the electric and magnetic fields at values of r far from the dipole are given by

$$\begin{aligned} \mathbf{E} &= -\frac{\beta^2 I_0 dl \sin \theta}{4\pi\epsilon\omega r} \sin(\omega t - \beta r) \mathbf{a}_\theta \\ &= -\frac{\eta\beta I_0 dl \sin \theta}{4\pi r} \sin(\omega t - \beta r) \mathbf{a}_\theta \end{aligned} \quad (10.17a)$$

$$\mathbf{H} = -\frac{\beta I_0 dl \sin \theta}{4\pi r} \sin(\omega t - \beta r) \mathbf{a}_\phi \quad (10.17b)$$

These fields are known as the *radiation fields*, since they are the components of the total fields that contribute to the time-average radiated power away from the dipole. Before we discuss the nature of these fields, let us find out quantitatively what we mean by *far from the dipole*. To do this, we look at the expression for the complete magnetic field given by (10.9) and note that the ratio of the amplitudes of the $1/r^2$ and $1/r$ terms is equal to $1/\beta r$. Hence, for $\beta r \gg 1$, the $1/r^2$ term is negligible compared to the $1/r$ term, as already pointed out in the previous section. This means that for $r \gg 1/\beta$, or $r \gg \lambda/2\pi$, that is, even at a distance of a few wavelengths from the dipole, the fields are predominantly radiation fields.

Returning now to the expressions for the radiation fields given by (10.17a) and (10.17b), we note that at any given point, (1) the electric field (E_θ), the magnetic field (H_ϕ) and the direction of propagation (r) are mutually perpendicular, and (2) the ratio of E_θ to H_ϕ is equal to η , which are characteristic of uniform plane waves. The phase of the field, however, is uniform over the surfaces $r = \text{constant}$, that is, spherical surfaces centered at the dipole, whereas the amplitude of the field is uniform over surfaces $(\sin \theta)/r = \text{constant}$. Hence, the fields are only locally uniform plane waves, that is, over any small area normal to the r -direction at a given point.

The Poynting vector due to the radiation fields is given by

$$\begin{aligned}
 \mathbf{P} &= \mathbf{E} \times \mathbf{H} \\
 &= E_\theta \mathbf{a}_\theta \times H_\phi \mathbf{a}_\phi = E_\theta H_\phi \mathbf{a}_r \\
 &= \frac{\eta \beta^2 I_0^2 (dl)^2 \sin^2 \theta}{16\pi^2 r^2} \sin^2(\omega t - \beta r) \mathbf{a}_r
 \end{aligned} \tag{10.18}$$

By evaluating the surface integral of the Poynting vector over any surface enclosing the dipole, we can find the power flow out of that surface, that is, the power “radiated” by the dipole. For convenience in evaluating the surface integral, we choose the spherical surface of radius r and centered at the dipole, as shown in Fig. 10.4. Thus, noting that the differential surface area on the spherical surface is $(r d\theta)(r \sin \theta d\phi) \mathbf{a}_r$ or $r^2 \sin \theta d\theta d\phi \mathbf{a}_r$, we obtain the instantaneous power radiated to be

$$\begin{aligned}
 P_{\text{rad}} &= \int_{\theta=0}^{\pi} \int_{\phi=0}^{2\pi} \mathbf{P} \cdot r^2 \sin \theta d\theta d\phi \mathbf{a}_r \\
 &= \int_{\theta=0}^{\pi} \int_{\phi=0}^{2\pi} \frac{\eta \beta^2 I_0^2 (dl)^2 \sin^3 \theta}{16\pi^2} \sin^2(\omega t - \beta r) d\theta d\phi \\
 &= \frac{\eta \beta^2 I_0^2 (dl)^2}{8\pi} \sin^2(\omega t - \beta r) \int_{\theta=0}^{\pi} \sin^3 \theta d\theta \\
 &= \frac{\eta \beta^2 I_0^2 (dl)^2}{6\pi} \sin^2(\omega t - \beta r) \\
 &= \frac{2\pi \eta I_0^2}{3} \left(\frac{dl}{\lambda} \right)^2 \sin^2(\omega t - \beta r)
 \end{aligned} \tag{10.19}$$

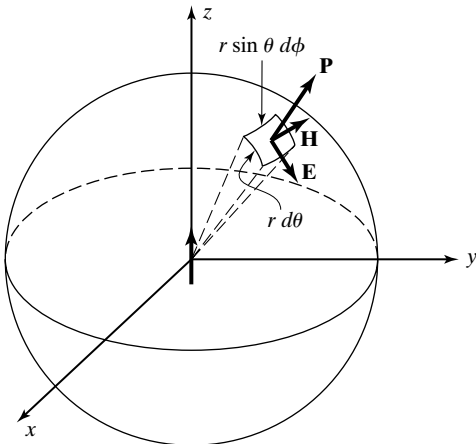


FIGURE 10.4

For computing the power radiated by the Hertzian dipole.

The time-average power radiated by the dipole, that is, the average of P_{rad} over one period of the current variation, is

$$\begin{aligned}\langle P_{\text{rad}} \rangle &= \frac{2\pi\eta I_0^2}{3} \left(\frac{dl}{\lambda} \right)^2 \langle \sin^2(\omega t - \beta r) \rangle \\ &= \frac{\pi\eta I_0^2}{3} \left(\frac{dl}{\lambda} \right)^2 \\ &= \frac{1}{2} I_0^2 \left[\frac{2\pi\eta}{3} \left(\frac{dl}{\lambda} \right)^2 \right]\end{aligned}\quad (10.20)$$

*Radiation
resistance*

We now define a quantity known as the *radiation resistance* of the antenna, denoted by the symbol R_{rad} , as the value of a fictitious resistor that dissipates the same amount of time-average power as that radiated by the antenna when a current of the same peak amplitude as that in the antenna is passed through it. Recalling that the average power dissipated in a resistor R when a current $I_0 \cos \omega t$ is passed through it is $\frac{1}{2} I_0^2 R$, we note from (10.20) that the radiation resistance of the Hertzian dipole is

$$R_{\text{rad}} = \frac{2\pi\eta}{3} \left(\frac{dl}{\lambda} \right)^2 \Omega \quad (10.21)$$

For free space, $\eta = \eta_0 = 120\pi \Omega$, and

$$R_{\text{rad}} = 80\pi^2 \left(\frac{dl}{\lambda} \right)^2 \Omega \quad (10.22)$$

As a numerical example, for (dl/λ) equal to 0.01, $R_{\text{rad}} = 80\pi^2(0.01)^2 = 0.08 \Omega$. Thus, for a current of peak amplitude 1 A, the time-average radiated power is equal to 0.04 W. This indicates that a Hertzian dipole of length 0.01λ is not a very effective radiator.

We note from (10.21) that the radiation resistance and, hence, the radiated power are proportional to the square of the electrical length, that is, the physical length expressed in terms of wavelength, of the dipole. The result given by (10.21) is, however, valid only for small values of dl/λ since if dl/λ is not small, the amplitude of the current along the antenna can no longer be uniform and its variation must be taken into account in deriving the radiation fields and hence the radiation resistance. We shall do this in the following section for a half-wave dipole, that is, for a dipole of length equal to $\lambda/2$.

*Radiation
pattern*

Let us now examine the directional characteristics of the radiation from the Hertzian dipole. We note from (10.17a) and (10.17b) that, for a constant r , the amplitude of the fields is proportional to $\sin \theta$. Similarly, we note from (10.18) that for a constant r , the power density is proportional to $\sin^2 \theta$. Thus, an observer wandering on the surface of an imaginary sphere centered at the dipole views different

amplitudes of the fields and of the power density at different points on the surface. The situation is illustrated in Fig. 10.5(a) for the power density by attaching to different points on the spherical surface vectors having lengths proportional to the Poynting vectors at those points. It can be seen that the power density is largest for $\theta = \pi/2$, that is, in the plane normal to the axis of the dipole, and decreases continuously toward the axis of the dipole, becoming zero along the axis.

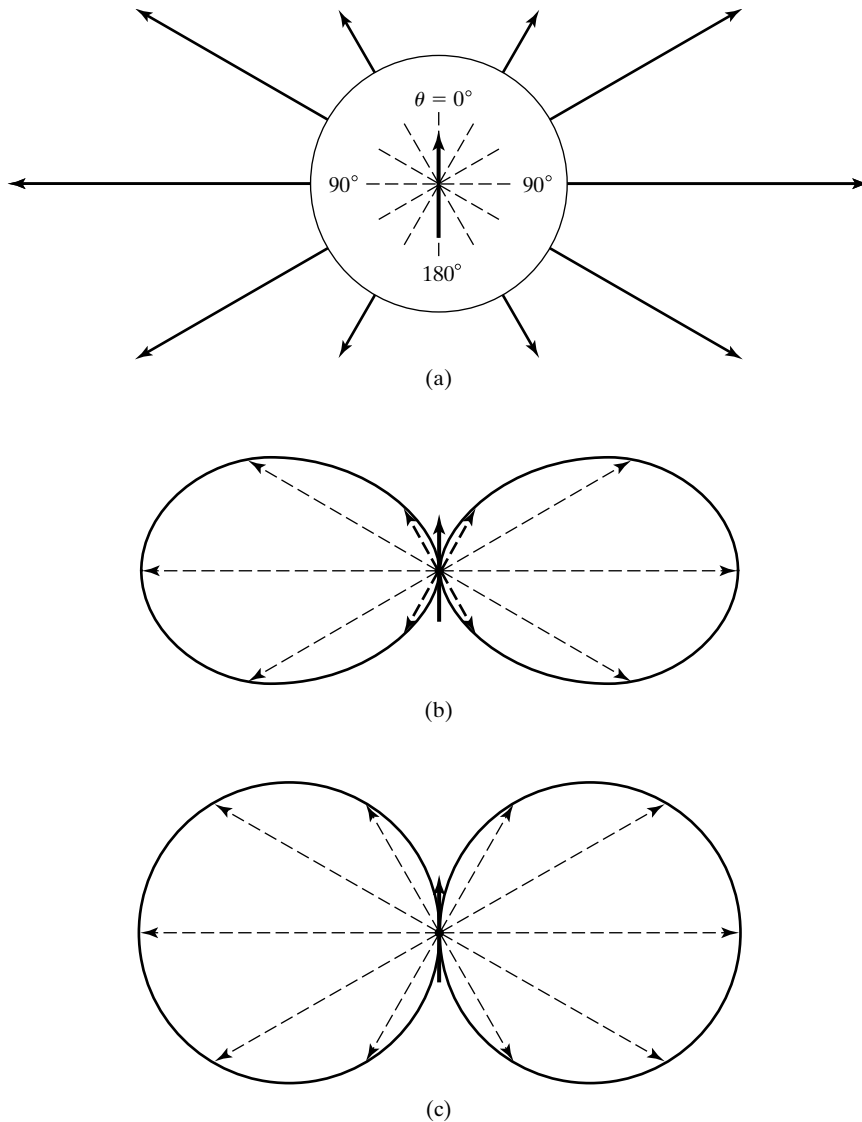


FIGURE 10.5
Directional characteristics of radiation from the Hertzian dipole.

It is customary to depict the radiation characteristic by means of a *radiation pattern*, as shown in Fig. 10.5(b), which can be imagined to be obtained by shrinking the radius of the spherical surface in Fig. 10.5(a) to zero with the Poynting vectors attached to it and then joining the tips of the Poynting vectors. Thus, the distance from the dipole point to a point on the radiation pattern is proportional to the power density in the direction of that point. Similarly, the radiation pattern for the fields can be drawn as shown in Fig. 10.5(c), based on the $\sin \theta$ dependence of the fields. In view of the independence of the fields from ϕ , the patterns of Figs. 10.5(b) and (c) are valid for any plane containing the axis of the dipole. In fact, the three-dimensional radiation patterns can be imagined to be the figures obtained by revolving these patterns about the dipole axis. For a general case, the radiation may also depend on ϕ , and hence it will be necessary to draw a radiation pattern for the $\theta = \pi/2$ plane. Here, this pattern is merely a circle centered at the dipole.

Directivity

We now define a parameter known as the *directivity* of the antenna, denoted by the symbol D , as the ratio of the maximum power density radiated by the antenna to the average power density. To elaborate on the definition of D , imagine that we take the power radiated by the antenna and distribute it equally in all directions by shortening some of the vectors in Fig. 10.5(a) and lengthening the others so that they all have equal lengths. The pattern then becomes nondirectional, and the power density, which is the same in all directions, will be less than the maximum power density of the original pattern. Obviously, the more directional the radiation pattern of an antenna is, the greater is the directivity.

From (10.18), we obtain the maximum power density radiated by the Hertzian dipole to be

$$\begin{aligned} [P_r]_{\max} &= \frac{\eta\beta^2 I_0^2 (dl)^2 [\sin^2 \theta]_{\max}}{16\pi^2 r^2} \sin^2(\omega t - \beta r) \\ &= \frac{\eta\beta^2 I_0^2 (dl)^2}{16\pi^2 r^2} \sin^2(\omega t - \beta r) \end{aligned} \quad (10.23)$$

By dividing the radiated power given by (10.19) by the surface area $4\pi r^2$ of the sphere of radius r , we obtain the average power density to be

$$[P_r]_{\text{av}} = \frac{P_{\text{rad}}}{4\pi r^2} = \frac{\eta\beta^2 I_0^2 (dl)^2}{24\pi^2 r^2} \sin^2(\omega t - \beta r) \quad (10.24)$$

Thus, the directivity of the Hertzian dipole is given by

$$D = \frac{[P_r]_{\max}}{[P_r]_{\text{av}}} = 1.5 \quad (10.25)$$

To generalize the computation of directivity for an arbitrary radiation pattern, let us consider

$$P_r = \frac{P_0 \sin^2(\omega t - \beta r)}{r^2} f(\theta, \phi) \quad (10.26)$$

where P_0 is a constant, and $f(\theta, \phi)$ is the power density pattern. Then

$$\begin{aligned}
 [P_r]_{\max} &= \frac{P_0 \sin^2(\omega t - \beta r)}{r^2} [f(\theta, \phi)]_{\max} \\
 [P_r]_{\text{av}} &= \frac{P_{\text{rad}}}{4\pi r^2} \\
 &= \frac{1}{4\pi r^2} \int_{\theta=0}^{2\pi} \int_{\phi=0}^{\pi} \frac{P_0 \sin^2(\omega t - \beta r)}{r^2} f(\theta, \phi) \mathbf{a}_r \cdot r^2 \sin \theta \, d\theta \, d\phi \, \mathbf{a}_r \\
 &= \frac{P_0 \sin^2(\omega t - \beta r)}{4\pi r^2} \int_{\theta=0}^{\pi} \int_{\phi=0}^{2\pi} f(\theta, \phi) \sin \theta \, d\theta \, d\phi \\
 \boxed{D} &= 4\pi \frac{[f(\theta, \phi)]_{\max}}{\int_{\theta=0}^{\pi} \int_{\phi=0}^{2\pi} f(\theta, \phi) \sin \theta \, d\theta \, d\phi} \quad (10.27)
 \end{aligned}$$

Example 10.2 Computation of directivity of an antenna for a given power density radiation pattern

Let us compute the directivity corresponding to the power density pattern function $f(\theta, \phi) = \sin^2 \theta \cos^2 \theta$.

From (10.27),

$$\begin{aligned}
 D &= 4\pi \frac{[\sin^2 \theta \cos^2 \theta]_{\max}}{\int_{\theta=0}^{\pi} \int_{\phi=0}^{2\pi} \sin^3 \theta \cos^2 \theta \, d\theta \, d\phi} \\
 &= 4\pi \frac{[\frac{1}{4} \sin^2 2\theta]_{\max}}{2\pi \int_{\theta=0}^{\pi} (\sin^3 \theta - \sin^5 \theta) \, d\theta} \\
 &= \frac{1}{2} \frac{1}{(4/3) - (16/15)} \\
 &= 1 \frac{7}{8}
 \end{aligned}$$

The ratio of the power density radiated by the antenna as a function of direction to the average power density is given by $Df(\theta, \phi)$. This quantity is known as the *directive gain of the antenna*. Another useful parameter is the power gain of the antenna, which takes into account the ohmic power losses in the antenna. It is denoted by the symbol G and is proportional to the directive gain, the proportionality factor being the power efficiency of the antenna, which is the ratio of the power radiated by the antenna to the power supplied to it by the source of excitation.

- K10.2.** Radiation fields; $\beta r \gg 1$; $1/r$ terms; Time-average radiated power; Radiation resistance; Radiation pattern; Power density; Directivity.
- D10.3.** Three Hertzian dipoles of lengths 1, 2, and 2 m are situated at the origin oriented along the positive x -, y -, and z -axes, respectively, carrying currents $1 \cos 2\pi \times 10^6 t$, $2 \cos 2\pi \times 10^6 t$, and $2 \sin 2\pi \times 10^6 t$ A, respectively. Determine the polarizations (including right-hand or left-hand sense in the case of circular and elliptical) of the radiation field at each of the following points: **(a)** a point on the x -axis; **(b)** a point on the y -axis; and **(c)** a point on the z -axis.
Ans. **(a)** right circular; **(b)** left elliptical; **(c)** linear.
- D10.4.** Compute the directivity corresponding to each of the following functions $f(\theta, \phi)$ in (10.27):

$$\begin{aligned} \text{(a)} \quad f(\theta, \phi) &= \begin{cases} 1 & \text{for } 0 < \theta < \pi/2 \\ 0 & \text{otherwise} \end{cases} \\ \text{(b)} \quad f(\theta, \phi) &= \begin{cases} \sin^2 \theta & \text{for } 0 < \theta < \pi/2 \\ 0 & \text{otherwise} \end{cases} \\ \text{(c)} \quad f(\theta, \phi) &= \begin{cases} 1 & \text{for } 0 < \theta < \pi/2 \\ \sin^2 \theta & \text{for } \pi/2 < \theta < \pi \end{cases} \end{aligned}$$

Ans. **(a)** 2; **(b)** 3; **(c)** 1.2.

10.3 LINEAR ANTENNAS

In the preceding section, we found the radiation fields due to a Hertzian dipole, which is an elemental antenna of infinitesimal length. If we now have an antenna of any length having a specified current distribution, we can divide it into a series of Hertzian dipoles, and by applying superposition, we can find the radiation fields for that antenna. We illustrate this procedure in this section by first considering the half-wave dipole, which is a commonly used form of antenna.

Half-wave dipole

The half-wave dipole is a center-fed, straight-wire antenna of length L equal to $\lambda/2$ and having the current distribution

$$I(z) = I_0 \cos \frac{\pi z}{L} \cos \omega t \quad \text{for } -L/2 < z < L/2 \quad (10.28)$$

where the dipole is assumed to be oriented along the z -axis with its center at the origin, as shown in Fig. 10.6(a). As can be seen from Fig. 10.6(a), the amplitude of the current distribution varies sinusoidally along the antenna with zeros at the ends and maximum at the center. To see how this distribution comes about, the half-wave dipole may be imagined to be the evolution of an open-circuited transmission line with the conductors folded perpendicularly to the line at points $\lambda/4$ from the end of the line. The current standing wave pattern for an open-circuited line is shown in Fig. 10.6(b). It consists of zero current at the open circuit and maximum current at $\lambda/4$ from the open circuit, that is, at points a and a' . Hence, it can be seen that when the conductors are folded perpendicularly to the line at a and a' , the half-wave dipole shown in Fig. 10.6(a) results.

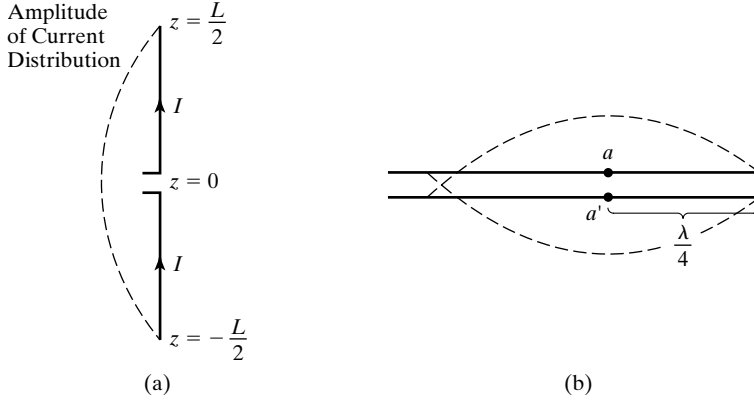


FIGURE 10.6

(a) Half-wave dipole. (b) Open-circuited transmission line for illustrating the evolution of the half-wave dipole.

Now to find the radiation field due to the half-wave dipole, we divide it into a number of Hertzian dipoles, each of length dz' , as shown in Fig. 10.7. If we consider one of these dipoles situated at distance z' from the origin, then from (10.28), the current in this dipole is $I_0 \cos(\pi z'/L) \cos \omega t$. From (10.17a) and (10.17b), the radiation fields due to this dipole at point P situated at distance r' from it are given by

$$d\mathbf{E} = -\frac{\eta\beta I_0 \cos(\pi z'/L) dz' \sin \theta'}{4\pi r'} \sin(\omega t - \beta r') \mathbf{a}_{\theta'} \quad (10.29a)$$

$$d\mathbf{H} = -\frac{\beta I_0 \cos(\pi z'/L) dz' \sin \theta'}{4\pi r'} \sin(\omega t - \beta r') \mathbf{a}_{\phi} \quad (10.29b)$$

where θ' is the angle between the z -axis and the line from the current element to the point P and $\mathbf{a}_{\theta'}$ is the unit vector perpendicular to that line, as shown in Fig. 10.7. The fields due to the entire current distribution of the half-wave dipole are then given by

$$\begin{aligned} \mathbf{E} &= \int_{z'=-L/2}^{L/2} d\mathbf{E} \\ &= -\int_{z'=-L/2}^{L/2} \frac{\eta\beta I_0 \cos(\pi z'/L) \sin \theta' dz'}{4\pi r'} \sin(\omega t - \beta r') \mathbf{a}_{\theta'} \end{aligned} \quad (10.30a)$$

$$\begin{aligned} \mathbf{H} &= \int_{z'=-L/2}^{L/2} d\mathbf{H} \\ &= -\int_{z'=-L/2}^{L/2} \frac{\beta I_0 \cos(\pi z'/L) \sin \theta' dz'}{4\pi r'} \sin(\omega t - \beta r') \mathbf{a}_{\phi} \end{aligned} \quad (10.30b)$$

where r' , θ' , and $\mathbf{a}_{\theta'}$ are functions of z' .

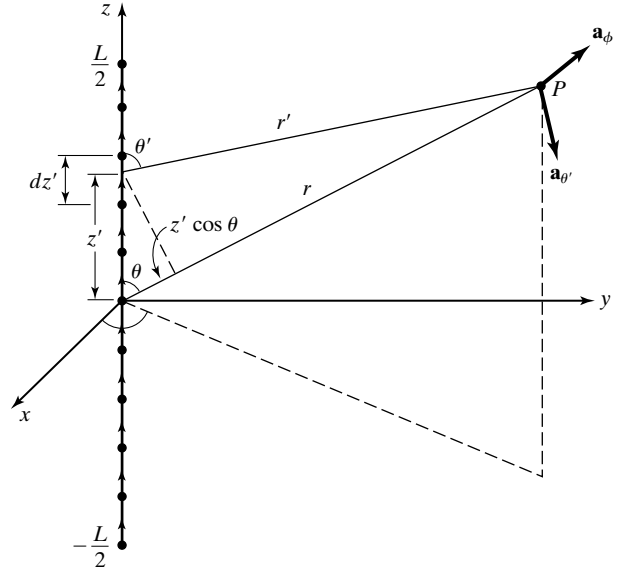


FIGURE 10.7

For the determination of the radiation field due to the half-wave dipole.

For radiation fields, r' is at least equal to several wavelengths and hence $\gg L$. We can therefore set $\mathbf{a}_{\theta'} \approx \mathbf{a}_{\theta}$ and $\theta' \approx \theta$ since they do not vary significantly for $-L/2 < z' < L/2$. We can also set $r' \approx r$ in the amplitude factors for the same reason, but for r' in the phase factors, we substitute $r - z' \cos \theta$ since the phase angle in $\sin(\omega t - \beta r')$ can vary appreciably over the range $-L/2 < z' < L/2$. For example, if $L = 2 \text{ m}$ ($\lambda = 4 \text{ m}$), $\theta = 0$, and $r = 10$, then r' varies from 11 for $z' = -L/2$ to 9 for $z' = L/2$, and $\pi r'/L$ varies from 5.5π for $z' = -L/2$ to 4.5π for $z' = L/2$. Thus, we have

$$\mathbf{E} = E_{\theta} \mathbf{a}_{\theta}$$

where

$$\begin{aligned} E_{\theta} &= - \int_{z'=-L/2}^{L/2} \frac{\eta \beta I_0 \cos(\pi z'/L) \sin \theta}{4\pi r} \sin(\omega t - \beta r + \beta z' \cos \theta) dz' \\ &= - \frac{\eta(\pi/L) I_0 \sin \theta}{4\pi r} \int_{z'=-L/2}^{L/2} \cos \frac{\pi z'}{L} \sin \left(\omega t - \frac{\pi}{L} r + \frac{\pi}{L} z' \cos \theta \right) dz' \end{aligned}$$

Evaluating the integral, we obtain

$$E_{\theta} = - \frac{\eta I_0 \cos[(\pi/2) \cos \theta]}{2\pi r \sin \theta} \sin \left(\omega t - \frac{\pi}{L} r \right) \quad (10.31a)$$

Similarly,

$$\mathbf{H} = H_\phi \mathbf{a}_\phi$$

where

$$H_\phi = -\frac{I_0}{2\pi r} \frac{\cos[(\pi/2) \cos \theta]}{\sin \theta} \sin\left(\omega t - \frac{\pi}{L} r\right) \quad (10.31b)$$

The Poynting vector due to the radiation fields of the half-wave dipole is given by

$$\begin{aligned} \mathbf{P} &= \mathbf{E} \times \mathbf{H} = E_\theta H_\phi \mathbf{a}_r \\ &= \frac{\eta I_0^2}{4\pi^2 r^2} \frac{\cos^2[(\pi/2) \cos \theta]}{\sin^2 \theta} \sin^2\left(\omega t - \frac{\pi}{L} r\right) \mathbf{a}_r \end{aligned} \quad (10.32)$$

The power radiated by the half-wave dipole is given by

$$\begin{aligned} P_{\text{rad}} &= \int_{\theta=0}^{\pi} \int_{\phi=0}^{2\pi} \mathbf{P} \cdot \mathbf{r}^2 \sin \theta \, d\theta \, d\phi \, \mathbf{a}_r \\ &= \int_{\theta=0}^{\pi} \int_{\phi=0}^{2\pi} \frac{\eta I_0^2}{4\pi^2} \frac{\cos^2[(\pi/2) \cos \theta]}{\sin \theta} \sin^2\left(\omega t - \frac{\pi}{L} r\right) d\theta \, d\phi \quad (10.33) \\ &= \frac{\eta I_0^2}{\pi} \sin^2\left(\omega t - \frac{\pi}{L} r\right) \int_{\theta=0}^{\pi/2} \frac{\cos^2[(\pi/2) \cos \theta]}{\sin \theta} d\theta \\ &= \frac{0.609 \eta I_0^2}{\pi} \sin^2\left(\omega t - \frac{\pi}{L} r\right) \end{aligned}$$

where we have used the result

$$\int_{\theta=0}^{\pi/2} \frac{\cos^2[(\pi/2) \cos \theta]}{\sin \theta} d\theta = 0.609$$

obtainable by numerical integration. The time-average radiated power is

$$\begin{aligned} \langle P_{\text{rad}} \rangle &= \frac{0.609 \eta I_0^2}{\pi} \left\langle \sin^2\left(\omega t - \frac{\pi}{L} r\right) \right\rangle \\ &= \frac{1}{2} I_0^2 \left(\frac{0.609 \eta}{\pi} \right) \end{aligned} \quad (10.34)$$

Thus, the radiation resistance of the half-wave dipole is

$$R_{\text{rad}} = \frac{0.609 \eta}{\pi} \Omega \quad (10.35)$$

For free space, $\eta = \eta_0 = 120\pi \Omega$, and

$$R_{\text{rad}} = 0.609 \times 120 = 73\Omega \tag{10.36}$$

Turning our attention now to the directional characteristics of the half-wave dipole, we note from (10.31a) and (10.31b) that the radiation pattern for the fields is $\{\cos [(\pi/2) \cos \theta]\}/\sin \theta$, whereas for the power density, it is $\{\cos^2 [(\pi/2) \cos \theta]\}/\sin^2 \theta$. These patterns, shown in Fig. 10.8(a) and (b), are slightly more directional than the corresponding patterns for the Hertzian dipole. The directivity of the half-wave dipole may now be found by using (10.27). Thus,

$$D = 4\pi \frac{\{\cos^2 [(\pi/2) \cos \theta]/\sin^2 \theta\}_{\text{max}}}{\int_{\theta=0}^{\pi} \int_{\phi=0}^{2\pi} \{\cos^2 [(\pi/2) \cos \theta]/\sin^2 \theta\} \sin \theta \, d\theta \, d\phi}$$

$$= 4\pi \frac{1}{2\pi \times 2 \times 0.609}$$

or

$$D = 1.642 \tag{10.37}$$

Linear antenna of arbitrary length

For a center-fed linear antenna of length L equal to an arbitrary number of wavelengths, the current distribution can be written as

$$I(z) = \begin{cases} I_0 \sin \beta \left(\frac{L}{2} + z \right) \cos \omega t & \text{for } -\frac{L}{2} < z < 0 \\ I_0 \sin \beta \left(\frac{L}{2} - z \right) \cos \omega t & \text{for } 0 < z < \frac{L}{2} \end{cases} \tag{10.38}$$

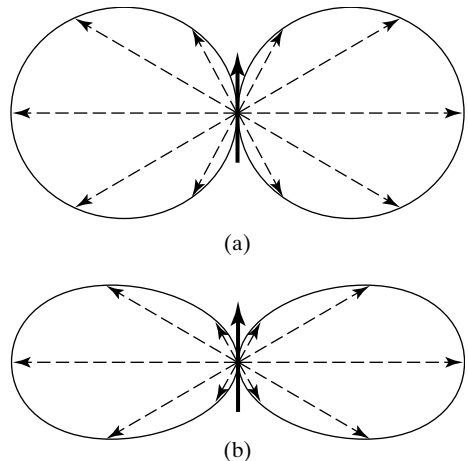


FIGURE 10.8 Radiation patterns for (a) the fields and (b) the power density due to the half-wave dipole.

where once again the antenna is assumed to be oriented along the z -axis with its center at the origin. Note that the current distribution is such that the amplitude of the current goes to zero at the two ends of the antenna and varies sinusoidally along the antenna with phase reversals every half wavelength from the ends, as shown, for example, for $L = 5\lambda/2$ in Fig. 10.9. Note also that for $L = \lambda/2$, (10.38) reduces to (10.28). Using (10.38) and proceeding in the same manner as for the half-wave dipole, the components of the radiation fields, the radiation resistance, and the directivity for the linear antenna of arbitrary electrical length can be obtained. The results are

$$E_\theta = -\frac{\eta I_0}{2\pi r} F(\theta) \sin(\omega t - \beta r) \tag{10.39a}$$

$$H_\phi = -\frac{I_0}{2\pi r} F(\theta) \sin(\omega t - \beta r) \tag{10.39b}$$

$$R_{\text{rad}} = \frac{\eta}{\pi} \int_{\theta=0}^{\pi/2} F^2(\theta) \sin \theta \, d\theta \tag{10.39c}$$

$$D = \frac{[F^2(\theta)]_{\text{max}}}{\int_{\theta=0}^{\pi/2} F^2(\theta) \sin \theta \, d\theta} \tag{10.39d}$$

where

$$F(\theta) = \frac{\cos[(\beta L/2) \cos \theta] - \cos(\beta L/2)}{\sin \theta} \tag{10.40}$$

is the radiation pattern for the fields. For $L = k\lambda$, (10.40) reduces to

$$F(\theta) = \frac{\cos(k\pi \cos \theta) - \cos(k\pi)}{\sin \theta} \tag{10.41}$$

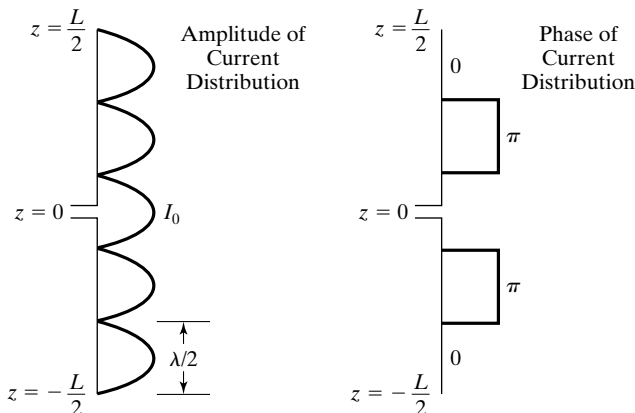


FIGURE 10.9 Variations of amplitude and phase of current distribution along a linear antenna of length $L = 5\lambda/2$.

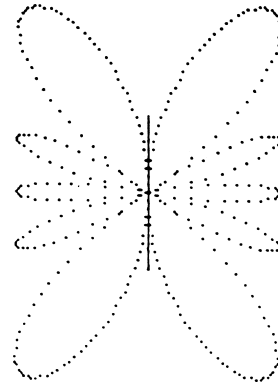


FIGURE 10.10

Computer-generated plot of radiation pattern for a linear antenna of length 2.5λ .

For a specified value of k , the radiation pattern can be obtained by substituting (10.41) for $0 < \theta < \pi$. As an example, Fig. 10.10 shows a computer-generated plot of the radiation pattern for $k = 2.5$. The radiation resistance and directivity can be computed by evaluating numerically the integrals in (10.39c) and (10.39d), respectively. For $k = 2.5$, these are 120.768 and 3.058, respectively.

- K10.3.** Half-wave dipole; Radiation fields; Radiation characteristics; Linear antenna; Arbitrary length.
- D10.5.** A center-fed linear antenna in free space has the current distribution of the form given by (10.38), where $I_0 = 1$ A. Find the amplitude of E_θ at $r = 100$ m for each of the following cases: **(a)** $L = 2$ m, $f = 75$ MHz, $\theta = 60^\circ$; **(b)** $L = 2$ m, $f = 200$ MHz, $\theta = 60^\circ$; and **(c)** $L = 4$ m, $f = 300$ MHz, $\theta = 30^\circ$.
- Ans.* **(a)** 0.49 V/m; **(b)** 0 V/m; **(c)** 1.335 V/m.

10.4 ANTENNA ARRAYS

In Section 3.5, we illustrated the principle of an antenna array by considering an array of two parallel, infinite plane, current sheets of uniform densities. We learned that by appropriately choosing the spacing between the current sheets and the amplitudes and phases of the current densities, a desired radiation characteristic can be obtained. The infinite plane current sheet is, however, a hypothetical antenna for which the fields are truly uniform plane waves propagating in the one dimension normal to the sheet. Now that we have gained some knowledge of physical antennas, in this section we consider arrays of such antennas.

The simplest array we can consider consists of two Hertzian dipoles, oriented parallel to the z -axis and situated at points on the x -axis on either side of and equidistant from the origin, as shown in Fig. 10.11. We shall consider the amplitudes of the currents in the two dipoles to be equal, but we shall allow a phase difference α between them. Thus, if $I_1(t)$ and $I_2(t)$ are the currents in the

*Array of two
Hertzian
dipoles*

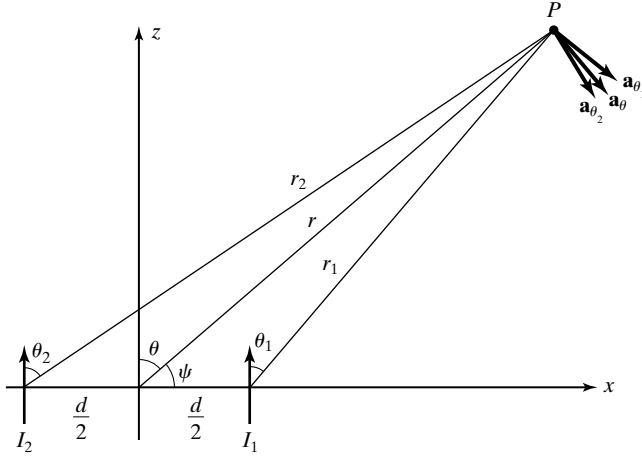


FIGURE 10.11
For computing the radiation field due to an array of two Hertzian dipoles.

dipoles situated at $(d/2, 0, 0)$ and $(-d/2, 0, 0)$, respectively, then

$$I_1 = I_0 \cos \left(\omega t + \frac{\alpha}{2} \right) \quad (10.42a)$$

$$I_2 = I_0 \cos \left(\omega t - \frac{\alpha}{2} \right) \quad (10.42b)$$

For simplicity, we consider a point P in the xz -plane and compute the radiation field at that point due to the array of the two dipoles. To do this, we note from (10.17a) that the electric field intensities at the point P due to the individual dipoles are given by

$$\mathbf{E}_1 = -\frac{\eta\beta I_0 dl \sin \theta_1}{4\pi r_1} \sin \left(\omega t - \beta r_1 + \frac{\alpha}{2} \right) \mathbf{a}_{\theta_1} \quad (10.43a)$$

$$\mathbf{E}_2 = -\frac{\eta\beta I_0 dl \sin \theta_2}{4\pi r_2} \sin \left(\omega t - \beta r_2 - \frac{\alpha}{2} \right) \mathbf{a}_{\theta_2} \quad (10.43b)$$

where $\theta_1, \theta_2, r_1, r_2, \mathbf{a}_{\theta_1}$, and \mathbf{a}_{θ_2} are as shown in Fig. 10.11.

For $r \gg d$, that is, for points far from the array, which is the region of interest, we can set $\theta_1 \approx \theta_2 \approx \theta$ and $\mathbf{a}_{\theta_1} \approx \mathbf{a}_{\theta_2} \approx \mathbf{a}_\theta$. Also, we can set $r_1 \approx r_2 \approx r$ in the amplitude factors, but for r_1 and r_2 in the phase factors, we substitute

$$r_1 \approx r - \frac{d}{2} \cos \psi \quad (10.44a)$$

$$r_2 \approx r + \frac{d}{2} \cos \psi \quad (10.44b)$$

where ψ is the angle made by the line from the origin to P with the axis of the array, that is, the x -axis, as shown in Fig. 10.11. Thus, we obtain the resultant field to be

$$\begin{aligned}
 \mathbf{E} &= \mathbf{E}_1 + \mathbf{E}_2 \\
 &= -\frac{\eta\beta I_0 dl \sin \theta}{4\pi r} \left[\sin\left(\omega t - \beta r + \frac{\beta d}{2} \cos \psi + \frac{\alpha}{2}\right) \right. \\
 &\quad \left. + \sin\left(\omega t - \beta r - \frac{\beta d}{2} \cos \psi - \frac{\alpha}{2}\right) \right] \mathbf{a}_\theta \\
 &= -\frac{2\eta\beta I_0 dl \sin \theta}{4\pi r} \cos\left(\frac{\beta d \cos \psi + \alpha}{2}\right) \sin(\omega t - \beta r) \mathbf{a}_\theta
 \end{aligned} \tag{10.45}$$

Unit, group, and resultant patterns

Comparing (10.45) with the expression for the electric field at P due to a single dipole situated at the origin, we note that the resultant field of the array is simply equal to the single dipole field multiplied by the factor $2 \cos [(\beta d \cos \psi + \alpha)/2]$, known as the *array factor*. Thus, the radiation pattern of the resultant field is given by the product of $\sin \theta$, which is the radiation pattern of the single dipole field, and $\cos [(\beta d \cos \psi + \alpha)/2]$, which is the radiation pattern of the array if the antennas were isotropic. We shall call these three patterns the *resultant pattern*, the *unit pattern*, and the *group pattern*, respectively. It is apparent that the group pattern is independent of the nature of the individual antennas as long as they have the same spacing and carry currents having the same relative amplitudes and phase differences. It can also be seen that the group pattern is the same in any plane containing the axis of the array. In other words, the three-dimensional group pattern is simply the pattern obtained by revolving the group pattern in the xz -plane about the x -axis, that is, the axis of the array.

Example 10.3 Group patterns for several cases of an array of two antennas

For the array of two antennas carrying currents having equal amplitudes, let us consider several pairs of d and α and investigate the group patterns.

Case 1: $d = \lambda/2, \alpha = 0$. The group pattern is

$$\left| \cos\left(\frac{\beta\lambda}{4} \cos \psi\right) \right| = \cos\left(\frac{\pi}{2} \cos \psi\right)$$

This is shown in Fig. 10.12(a). It has maxima perpendicular to the axis of the array and nulls along the axis of the array. Such a pattern is known as a *broadside pattern*.

Case 2: $d = \lambda/2, \alpha = \pi$. The group pattern is

$$\left| \cos\left(\frac{\beta\lambda}{4} \cos \psi + \frac{\pi}{2}\right) \right| = \left| \sin\left(\frac{\pi}{2} \cos \psi\right) \right|$$

This is shown in Fig. 10.12(b). It has maxima along the axis of the array and nulls perpendicular to the axis of the array. Such a pattern is known as an *endfire pattern*.

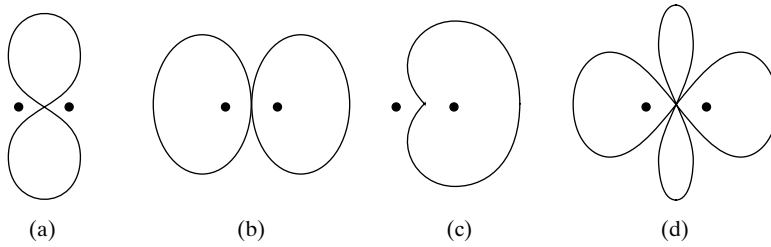


FIGURE 10.12

Group patterns for an array of two antennas carrying currents of equal amplitude for (a) $d = \lambda/2$, $\alpha = 0$, (b) $d = \lambda/2$, $\alpha = \pi$, (c) $d = \lambda/4$, $\alpha = -\pi/2$, and (d) $d = \lambda$, $\alpha = 0$.

Case 3: $d = \lambda/4$, $\alpha = -\pi/2$. The group pattern is

$$\left| \cos\left(\frac{\beta\lambda}{8} \cos \psi - \frac{\pi}{4}\right) \right| = \cos\left(\frac{\pi}{4} \cos \psi - \frac{\pi}{4}\right)$$

This is shown in Fig. 10.12(c). It has a maximum along $\psi = 0$ and null along $\psi = \pi$. Again, this is an endfire pattern, but directed to one side. This case is the same as the one considered in Section 3.5.

Case 4: $d = \lambda$, $\alpha = 0$. The group pattern is

$$\left| \cos\left(\frac{\beta\lambda}{2} \cos \psi\right) \right| = |\cos(\pi \cos \psi)|$$

This is shown in Fig. 10.12(d). It has maxima along $\psi = 0^\circ$, 90° , and 180° and nulls along $\psi = 60^\circ$ and 120° .

Proceeding further, we can obtain the resultant pattern for an array of two Hertzian dipoles by multiplying the unit pattern by the group pattern. Thus, recalling that the unit pattern for the Hertzian dipole is $\sin \theta$ in the plane of the dipole and considering values of $\lambda/2$ and 0 for d and α , respectively, for which the group pattern is given in Fig. 10.12(a), we obtain the resultant pattern in the xz -plane, as shown in Fig. 10.13(a). In the

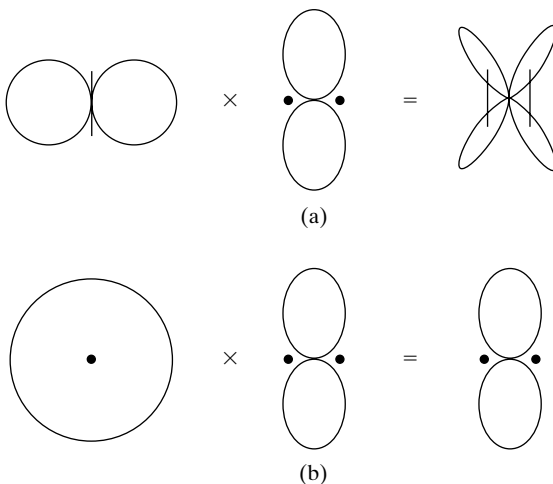


FIGURE 10.13

Determination of the resultant pattern of an antenna array by multiplication of unit and group patterns.

xy -plane, that is, the plane normal to the axis of the dipole, the unit pattern is a circle, and, hence, the resultant pattern is the same as the group pattern, as illustrated in Fig. 10.13(b).

Example 10.4 Pattern multiplication technique for obtaining the resultant pattern of an antenna array

Pattern multiplication

The procedure of multiplication of the unit and group patterns to obtain the resultant pattern illustrated in Example 10.3 is known as the *pattern multiplication* technique. Let us consider a linear array of four isotropic antennas spaced $\lambda/2$ apart and fed in phase, as shown in Fig. 10.14(a), and obtain the resultant pattern by using the pattern multiplication technique.

To obtain the resultant pattern of the four-element array, we replace it by a two-element array of spacing λ , as shown in Fig. 10.14(b), in which each element forms a unit representing a two-element array of spacing $\lambda/2$. The unit pattern is then the pattern shown in Fig. 10.12(a). The group pattern, which is the pattern of two isotropic radiators having $d = \lambda$ and $\alpha = 0$, is the pattern given in Fig. 10.12(d). The resultant pattern of the four-element array is the product of these two patterns, as illustrated in Fig. 10.14(c). If the individual elements of the four-element array are not isotropic, then this pattern becomes the group pattern for the determination of the new resultant pattern.

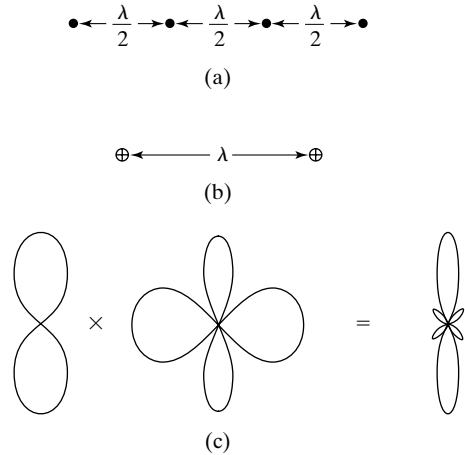


FIGURE 10.14 Determination of the resultant pattern for a linear array of four isotropic antennas.

Uniform linear array of n antennas

Let us now consider a uniform linear array of n antennas of spacing d , as shown in Fig. 10.15. Then assuming currents of equal amplitude I_0 and progressive phase shift α , that is, in the manner $I_0 \cos \omega t$, $I_0 \cos(\omega t + \alpha)$, $I_0 \cos(\omega t + 2\alpha)$, ... for antennas 1, 2, 3, ..., respectively, we can obtain the far field ($r \gg nd$) as follows. If the complex electric field at the point (r_0, ψ) due to element 1 is assumed to be $1e^{-j\beta r_0}$, then the complex electric fields at that point due to elements 2, 3, ...

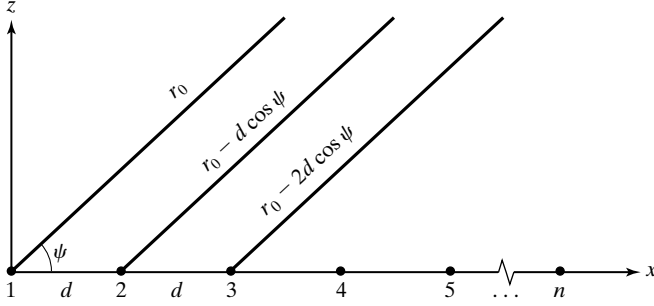


FIGURE 10.15

For obtaining the group pattern for a uniform linear array of n antennas.

are $1e^{j\alpha}e^{j\beta(r_0-d \cos \psi)}$, $1e^{j2\alpha}e^{j\beta(r_0-2d \cos \psi)}$, ..., so that the field due to the n -element array is

$$\begin{aligned}
 \bar{E}(\psi) &= 1e^{-j\beta r_0} + 1e^{j\alpha}e^{-j\beta(r_0-d \cos \psi)} \\
 &\quad + 1e^{j2\alpha}e^{-j\beta(r_0-2d \cos \psi)} + \dots \\
 &\quad + 1e^{j(n-1)\alpha}e^{-j\beta[r_0-(n-1)d \cos \psi]} \\
 &= [1 + e^{j(\beta d \cos \psi + \alpha)} + e^{j2(\beta d \cos \psi + \alpha)} \\
 &\quad + \dots + e^{j(n-1)(\beta d \cos \psi + \alpha)}]e^{-j\beta r_0} \\
 &= \frac{1 - e^{jn(\beta d \cos \psi + \alpha)}}{1 - e^{j(\beta d \cos \psi + \alpha)}}e^{-j\beta r_0}
 \end{aligned} \tag{10.46}$$

The magnitude of \bar{E} is given by

$$\begin{aligned}
 |\bar{E}(\psi)| &= \left| \frac{1 - e^{jn(\beta d \cos \psi + \alpha)}}{1 - e^{j(\beta d \cos \psi + \alpha)}} \right| \\
 &= \left| \frac{\sin n[(\beta d \cos \psi + \alpha)/2]}{\sin [(\beta d \cos \psi + \alpha)/2]} \right|
 \end{aligned} \tag{10.47}$$

which has a maximum value of n for $\beta d \cos \psi + \alpha = 0, 2\pi, 4\pi, \dots$. Thus, the group pattern is

$$F(\psi) = \frac{1}{n} \left| \frac{\sin n[(\beta d \cos \psi + \alpha)/2]}{\sin [(\beta d \cos \psi + \alpha)/2]} \right| \tag{10.48}$$

Note that for $n = 2$, (10.48) reduces to $\cos [(\beta d \cos \psi + \alpha)/2]$, which is the group pattern obtained for the two-element array. The nulls of the pattern occur for $n(\beta d \cos \psi + \alpha) = 2m\pi$, where m is any integer but not equal to 0, $n, 2n, \dots$. For $d = k\lambda$, (10.48) reduces to

$$F(\psi) = \frac{1}{n} \left| \frac{\sin n(\pi k \cos \psi + \alpha/2)}{\sin (\pi k \cos \psi + \alpha/2)} \right| \tag{10.49}$$

Figure 10.16 shows a computer-generated sequence of plots of F versus ψ ($0 \leq \psi \leq 180^\circ$) for values of α ranging from -180° to 150° in steps of 30° , for $n = 6$ and $k = 0.5$. It can be seen that as the value of α is varied, the value of ψ along which the principal maximum of the group pattern occurs varies in a continuous manner, as to be expected.

Principle of phased array

The behavior illustrated in Fig. 10.16 is the basis for the principle of phased arrays. In a phased array, the phase differences between the elements of the array are varied electronically to scan the radiation pattern over a desired angle without having to move the antenna structure mechanically.

Log-periodic dipole array

A type of array that is commonly seen is the *log-periodic dipole array*, which is an example of a broadband array. To discuss briefly, we first note that the directional properties of antennas and antenna arrays depend on their electrical dimensions, that is, the dimensions expressed in terms of the wavelength at the operating frequency. Hence, an antenna of fixed physical dimensions exhibits frequency-dependent characteristics. This very fact suggests that for an antenna to be frequency-independent, its electrical size must remain constant with frequency, and hence, its physical size should increase proportionately to the wavelength. Alternatively, for an antenna of fixed physical dimensions, the active region, that is, the region responsible for the predominant radiation, should vary with frequency, that is, scale itself in such a manner that its electrical size remains the same. An example in which this is the case is the log-periodic dipole array, shown in Fig. 10.17. As the name implies, it employs a number of

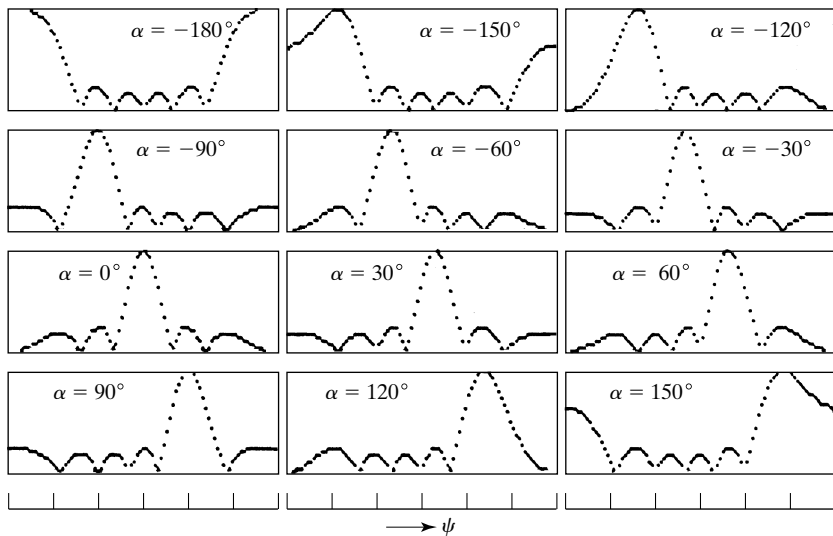


FIGURE 10.16

Plots of group patterns for the uniform linear array of Fig. 10.15 for $n = 6$ and $k = 0.5$. The horizontal scale for ψ for each plot is such that ψ varies for 0 to 180° .

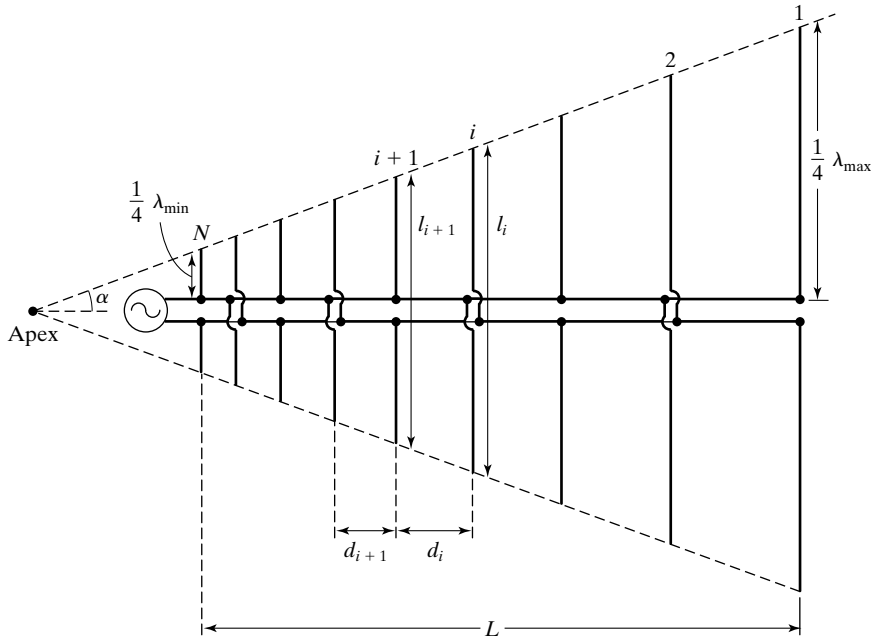


FIGURE 10.17

Log-periodic dipole array.

dipoles. The dipole lengths and the spacings between consecutive dipoles increase along the array by a constant scale factor such that

$$\frac{l_{i+1}}{l_i} = \frac{d_{i+1}}{d_i} = \tau \quad (10.50)$$

From the principle of scaling, it is evident that for this structure extending from zero to infinity and energized at the apex, the properties repeat at frequencies given by $\tau^n f$, where n takes integer values. When plotted on a logarithmic scale, these frequencies are equally spaced at intervals of $\log \tau$. It is for this reason that the structure is called *log periodic*.

The log-periodic dipole array is fed by a transmission line, as shown in Fig. 10.17, such that a 180° phase shift is introduced between successive elements in addition to that corresponding to the spacing between the elements. The resulting radiation pattern is directed toward the apex, that is, toward the source. Almost all the radiation takes place from those elements that are in the vicinity of a half wavelength long. The operating band of frequencies is therefore bounded on the low side by frequencies at which the largest elements are approximately a half wavelength long and on the high side by frequencies corresponding to the size of the smallest elements. As the frequency is varied, the radiating, or active, region moves back and forth along the array. Since practically all the input

power is radiated by the active region, the larger elements to the right of it are not excited. Furthermore, because the radiation is toward the apex, these larger elements are essentially in a field-free region and hence do not significantly influence the operation. Although the shorter elements to the left of the active region are in the antenna beam, they have small influence on the pattern because of their short lengths, close spacings, and the 180° phase shift.

K10.4. Antenna array; Unit pattern; Group pattern; Resultant pattern; Pattern multiplication; Uniform linear array; Image antenna concept; Corner reflector.

D10.6. For the array of two antennas of Example 10.3, assume that $d = 3\lambda/2$ and $\alpha = \pi/2$. Find the three lowest values of ψ for which the group pattern has nulls.

Ans. $33.56^\circ, 80.41^\circ, 120^\circ$.

D10.7. Obtain the expression for the resultant pattern for each of the following cases of linear array of isotropic antennas: **(a)** three antennas carrying currents with amplitudes in the ratio 1:2:1, spaced λ apart and fed in phase; **(b)** five antennas carrying currents with amplitudes in the ratio 1:2:2:2:1, spaced $\lambda/2$ apart and with progressive phase shift of 180° ; and **(c)** five antennas carrying currents in the ratio 1:2:3:2:1, spaced λ apart and fed in phase.

Ans. **(a)** $\cos^2(\pi \cos \psi)$; **(b)** $\sin^2[(\pi/2) \cos \psi] |\cos(\pi \cos \psi)|$;
(c) $[\sin^2(3\pi \cos \psi)]/[9 \sin^2(\pi \cos \psi)]$.

10.5 ANTENNAS IN THE PRESENCE OF REFLECTORS

Image antennas

Thus far, we have considered the antennas to be situated in an unbounded medium, so that the waves radiate in all directions from the antenna without giving rise to reflections from any obstacles. In practice, however, we have to consider the effect of reflections from the ground even if no other obstacles are present. To do this, it is reasonable to assume that the ground is a perfect conductor and use the concept of image antennas, which together with the actual antennas form arrays.

To introduce this concept, let us consider a Hertzian dipole oriented vertically and located at a height h above a plane, perfect conductor surface, as shown in Fig. 10.18(a). Since no waves can penetrate into the perfect conductor, as we learned in Section 4.5, the waves radiated from the dipole onto the conductor give rise to reflected waves, as shown in Fig. 10.18(a) for two directions of incidence. For a given incident wave onto the conductor surface, the angle of reflection is equal to the angle of incidence, as can be seen intuitively from the following reasons: (1) the reflected wave must propagate away from the conductor surface, (2) the apparent wavelengths of the incident and reflected waves parallel to the conductor surface must be equal, and (3) the tangential component of the resultant electric field on the conductor surface must be zero, which also determines the polarity of the reflected wave electric field. Also because of (3), the reflected wave amplitude must equal the incident wave amplitude. If we now extend the directions of propagation of the two reflected waves backward,

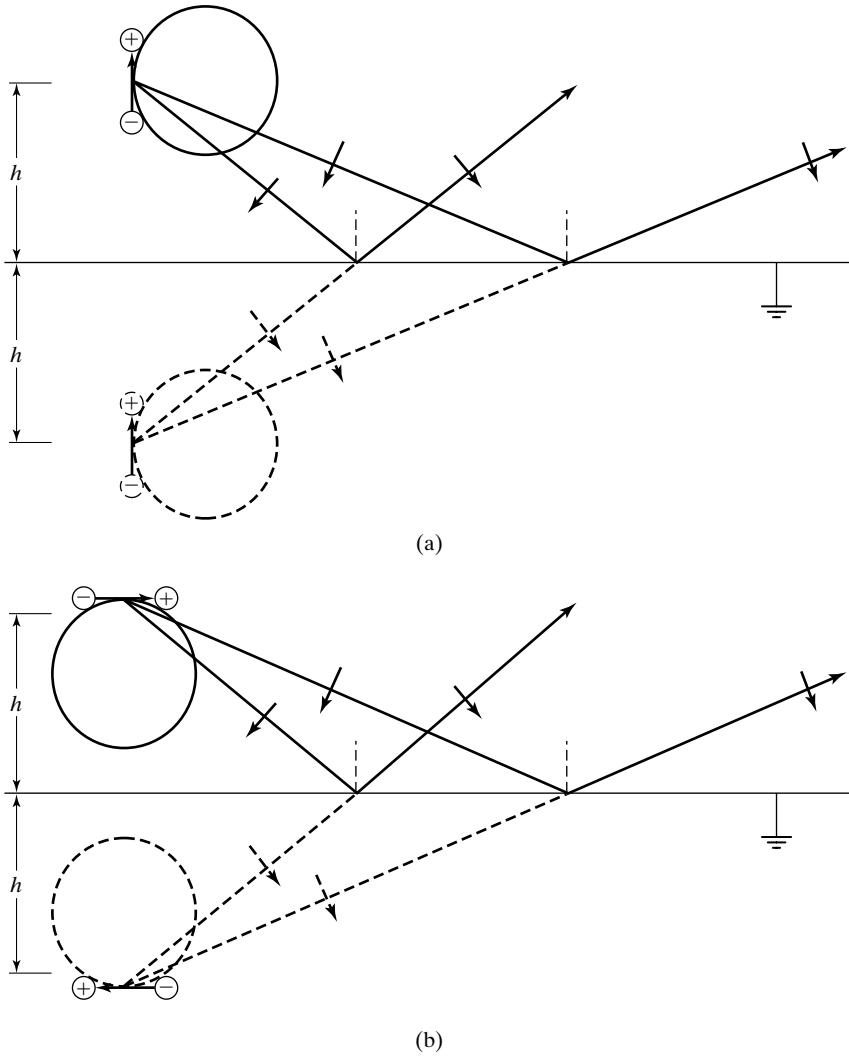


FIGURE 10.18

For illustrating the concept of image antennas. (a) Vertical Hertzian dipole and (b) horizontal Hertzian dipole above a plane perfect conductor surface.

they meet at a point that is directly beneath the dipole and at the same distance h below the conductor surface as the dipole is above it. Thus, the reflected waves appear to be originating from an antenna, which is the *image* of the actual antenna about the conductor surface. This image antenna must also be a vertical antenna since in order for the boundary condition of zero tangential electric field to be satisfied at all points on the conductor surface, the image antenna must have the same radiation pattern as that of the actual antenna, as shown in

Fig. 10.18(a). In particular, the current in the image antenna must be directed in the same sense as that in the actual antenna in order to be consistent with the polarity of the reflected wave electric field. It can be seen, therefore, that the charges associated with the image dipole have signs opposite to those of the corresponding charges associated with the actual dipole.

A similar reasoning can be applied to the case of a horizontal Hertzian dipole above a perfect conductor surface, as shown in Fig. 10.18(b). Here it can be seen that the current in the image antenna is directed in the opposite sense to that in the actual antenna. This again results in charges associated with the image dipole having signs opposite to those of the corresponding charges associated with the actual dipole. In fact, this is always the case.

From the foregoing discussion, it can be seen that the field due to an antenna in the presence of the conductor is the same as the resultant field of the array formed by the actual antenna and the image antenna. There is, of course, no field inside the conductor. The image antenna is only a virtual antenna that serves to simplify the field determination outside the conductor. The simplification results from the fact that we can use the knowledge gained on antenna arrays to determine the radiation pattern.

For example, for a vertical Hertzian dipole at a height of $\lambda/2$ above the conductor surface, the radiation pattern in the vertical plane is the product of the unit pattern, which is the radiation pattern of the single dipole in the plane of its axis, and the group pattern corresponding to an array of two isotropic radiators spaced λ apart and fed in phase. This multiplication and the resultant pattern are illustrated in Fig. 10.19. The radiation patterns for the case of the horizontal dipole can be obtained in a similar manner.

Corner reflector

To discuss another example of the application of the image-antenna concept, we consider the corner reflector, an arrangement of two plane perfect conductors at an angle to each other, as shown by the cross-sectional view in Fig. 10.20 for the case of the 90° angle. We shall assume that each conductor is semi-infinite in extent. For a Hertzian dipole situated parallel to both conductors, the locations and polarities of the images can be obtained to be as shown in the figure. By using the pattern multiplication technique, the radiation pattern in the cross-sectional plane can then be obtained.

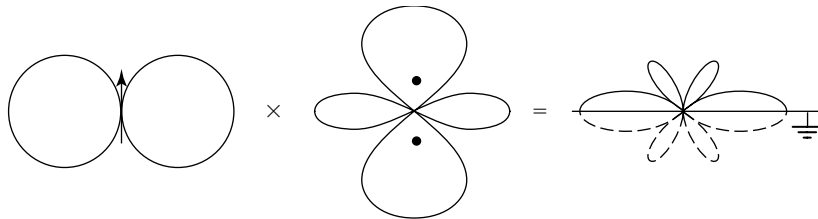


FIGURE 10.19

Determination of radiation pattern in the vertical plane for a vertical Hertzian dipole above a plane perfect conductor surface.

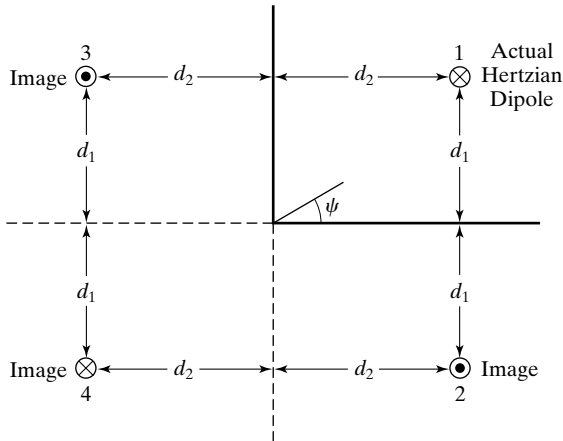


FIGURE 10.20

Application of image-antenna concept to obtain the radiation pattern for a Hertzian dipole in the presence of a corner reflector.

For an example, let $d_1 = d_2 = \lambda/4$. Then using the notation in Fig. 10.20, we can consider antennas 1 and 2 as constituting a unit for which the pattern is $|\sin [(\pi/2) \sin \psi]|$, which is that of case 2 in Example 10.3, except that ψ is measured from the line which is perpendicular to the axis of the array. Antennas 3 and 4 constitute a similar unit except for opposite polarity so that the group pattern for the two units is $|\sin [(\pi/2) \cos \psi]|$. Thus, the required radiation pattern is

$$\left| \sin \left(\frac{\pi}{2} \sin \psi \right) \sin \left(\frac{\pi}{2} \cos \psi \right) \right|$$

which is shown plotted in Fig. 10.21.

K10.5. Image antenna concept; Corner reflector.

D10.8. For the Hertzian dipole in the presence of the corner reflector of Fig. 10.20, let r be the ratio of the radiation field at a point in the cross-sectional plane and along the line extending from the corner through the dipole, to the radiation field at the same point in the absence of the corner reflector. Find the value of r for each of the following cases: **(a)** $d_1 = d_2 = \sqrt{2}\lambda$; **(b)** $d_1 = d_2 = \lambda/4\sqrt{2}$; and **(c)** $d_1 = 0.3\lambda$, $d_2 = 0.4\lambda$.

Ans. **(a)** 0; **(b)** 2; **(c)** 3.275.

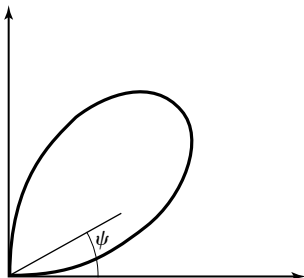


FIGURE 10.21

Radiation pattern in the cross-sectional plane for the case of $d_1 = d_2 = \lambda/4$ in the arrangement of Fig. 10.20.

10.6 APERTURE ANTENNAS

Description and examples

An important class of antennas, called *aperture antennas*, is one for which the radiation is computed from a knowledge of the field distribution in an aperture instead of from a current distribution associated with the source of radiation, as has been the case thus far. The corner reflector discussed in the previous section is, in the practical case of finite-sized conductors (and, hence, defining an aperture), an example of such an antenna. Besides reflectors such as the corner reflector, other examples of aperture antennas are horns extending from waveguides, slots in conducting enclosures, and lenses. Essentially for an aperture antenna, the primary source, which is elsewhere, sets up the field distribution in the aperture, which in turn is assumed to give rise to secondary waves in accordance with the Huygens-Fresnel principle, introduced in Section 9.6.

Far-field determination

In particular, as mentioned in Section 9.6, the determination of the far field from an aperture antenna is the same as setting up the problem to solve for Fraunhofer diffraction from the aperture. To review briefly, consider a plane monochromatic wave incident normally on a screen in the xy -plane, with an aperture cut into it, as shown in Fig. 10.22. Then, according to the Huygens-Fresnel principle, the incident wave may be thought of as giving rise to secondary (spherical) waves emanating from every point in the aperture and that interfere with one another to produce the field distribution away from the aperture. The scalar field at a point P is approximately given by

$$\bar{E}(P) \approx \frac{j\beta}{2\pi} \int_S \frac{\bar{E}(x', y', 0)}{R} e^{-j\beta R} dS \quad (10.51)$$

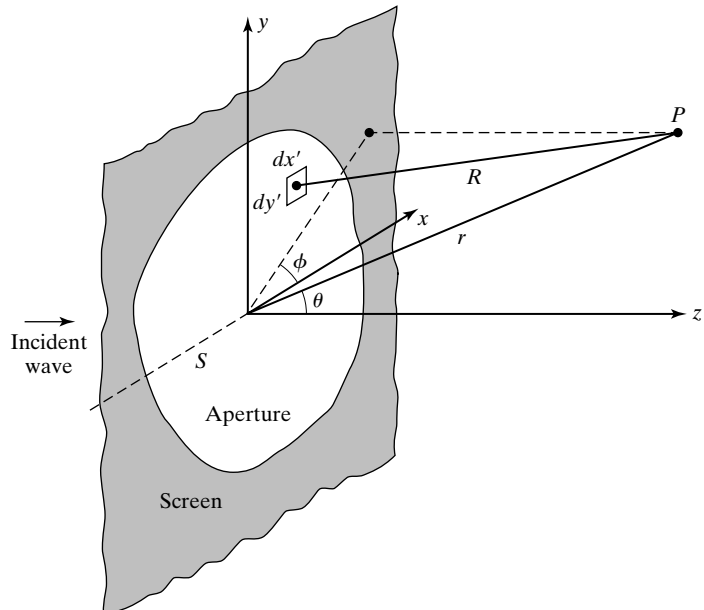


FIGURE 10.22

Geometry pertinent to the determination of the far field for radiation from an aperture antenna.

where S is the area of the aperture, and $\bar{E}(x', y', 0)$ is the scalar field in the aperture. For the Fraunhofer approximation, the waves arriving at P approach plane waves, thereby permitting simplification of the integrand in (10.51) by using the plane wave approximation. This consists of assuming that the lines from points in the aperture $(x', y', 0)$ to the observation point $P(x, y, z)$ are all parallel ($x', y' \ll r$), so that

$$\begin{aligned}
 R &= \sqrt{(x - x')^2 + (y - y')^2 + z^2} \\
 &= \sqrt{r^2 - 2xx' - 2yy' + (x')^2 + (y')^2} \\
 &= r \left[1 - \frac{2xx'}{r^2} - \frac{2yy'}{r^2} + \left(\frac{x'}{r}\right)^2 + \left(\frac{y'}{r}\right)^2 \right]^{1/2} \\
 &\approx r \left(1 - \frac{xx'}{r^2} - \frac{yy'}{r^2} \right) \\
 &= r - x' \sin \theta \cos \phi - y' \sin \theta \sin \phi
 \end{aligned} \tag{10.52}$$

For the R in the denominator in the integrand, further approximation can be made as $R \approx r$. Thus, (10.51) reduces to

$$\boxed{\bar{E}(x, y, z) \approx \frac{j\beta}{2\pi r} e^{-j\beta r} \int_S \bar{E}(x', y', 0) e^{j\beta \sin \theta (x' \cos \phi + y' \sin \phi)} dx' dy'} \tag{10.53}$$

Equation (10.53) is the starting point for the determination of the far-field distribution for an aperture antenna. We shall illustrate by means of an example.

Example 10.5 Far field for a rectangular-aperture antenna with uniform field distribution

Let us consider a rectangular aperture in the xy -plane and centered at the origin with a uniform field distribution $\bar{\mathbf{E}} = E_0 \mathbf{a}_y$ in it, as shown in Fig. 10.23, and investigate the characteristics of the far field due to it.

Rectangular aperture with uniform excitation

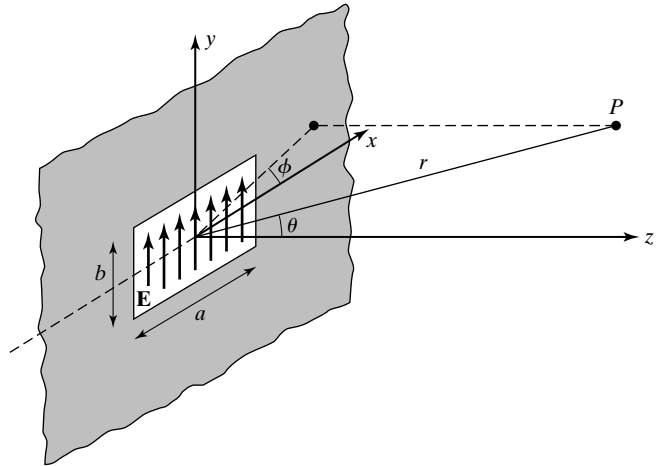
Applying (10.53) to the rectangular aperture, we have at a point $P(r, \theta, \phi)$ far from the aperture

$$\begin{aligned}
 \bar{E} &\approx \frac{j\beta e^{-j\beta r}}{2\pi r} \int_{x'=-a/2}^{a/2} \int_{y'=-b/2}^{b/2} E_0 e^{j\beta \sin \theta (x' \cos \phi + y' \sin \phi)} dx' dy' \\
 &= \frac{j\beta E_0 e^{-j\beta r}}{2\pi r} \int_{-a/2}^{a/2} e^{jx'\beta \sin \theta \cos \phi} dx' \int_{-b/2}^{b/2} e^{jy'\beta \sin \theta \sin \phi} dy'
 \end{aligned} \tag{10.54}$$

Evaluating the integrals, we obtain

$$\boxed{\bar{E} = \frac{j\beta E_0 a b e^{-j\beta r}}{2\pi r} \left(\frac{\sin \psi_1}{\psi_1} \right) \left(\frac{\sin \psi_2}{\psi_2} \right)} \tag{10.55}$$

FIGURE 10.23
Rectangular aperture antenna with a uniform field distribution in the aperture.



where

$$\psi_1 = \frac{\beta a \sin \theta \cos \phi}{2} \quad (10.56a)$$

and

$$\psi_2 = \frac{\beta b \sin \theta \sin \phi}{2} \quad (10.56b)$$

Radiation characteristics

The quantities of interest in (10.55) are the $(\sin \psi)/\psi$ type of terms, which determine the radiation pattern. To discuss this, we consider the two coordinate planes $\phi = 0$ and $\phi = 90^\circ$ and find from (10.55) that the amplitudes of the fields in these two planes are given by

$$\begin{aligned} |\bar{E}|_{\phi=0} &= \frac{\beta E_0 ab}{2\pi r} \left| \frac{\sin \psi_1}{\psi_1} \right|_{\phi=0} \\ &= \frac{\beta E_0 ab}{2\pi r} \left| \frac{\sin [(\beta a \sin \theta)/2]}{\beta a \sin \theta / 2} \right| \end{aligned} \quad (10.57a)$$

and

$$\begin{aligned} |\bar{E}|_{\phi=90^\circ} &= \frac{\beta E_0 ab}{2\pi r} \left| \frac{\sin \psi_2}{\psi_2} \right|_{\phi=90^\circ} \\ &= \frac{\beta E_0 ab}{2\pi r} \left| \frac{\sin [(\beta b \sin \theta)/2]}{\beta b \sin \theta / 2} \right| \end{aligned} \quad (10.57b)$$

where we have used the fact that $\lim_{\Delta \rightarrow 0} (\sin \Delta)/\Delta$ is equal to 1. Thus, in both planes, the behavior is the same except for the appearance of the different dimensions a and b in the $(\sin \psi)/\psi$ factors in (10.57a) and (10.57b), respectively.

To examine this behavior, we consider the plot of $|(\sin \psi)/\psi|$ versus ψ , which is shown in Fig. 10.24. We note that it indicates a strong central maximum of unity at $\psi = 0$ and a series of secondary (weaker) maxima on either side of it, with nulls occurring at $|\psi| = m\pi$, $m = 1, 2, 3, \dots$. The secondary maxima, which occur at $|\psi| = 1.4303\pi, 2.459\pi, 3.471\pi, \dots$, are successively less intense, having values 0.2172, 0.1284, 0.0913, \dots , respectively. If we consider the fact that the power density is proportional to $|\bar{E}|^2$, then the insignificance of these maxima becomes more evident, since the successive maxima of $|(\sin \psi)/\psi|^2$ are 1, 0.0472, 0.0165, 0.0083, \dots . Thus, the quantity of interest is the beam width between the first nulls (BWFN) between which the radiation is concentrated. The BWFN is given by twice the value of θ corresponding to the first null. For the $\phi = 0$ plane, this value is given by

$$\frac{\beta a \sin \theta}{2} = \pi \quad (10.58)$$

For narrow beams, which is the case in practice, $\sin \theta \approx \theta$ in this range, so that (10.58) can be written as

$$\begin{aligned} \frac{\beta a \theta}{2} &\approx \pi \\ \theta &\approx \frac{2\pi}{\beta a} = \frac{\lambda}{a} \end{aligned} \quad (10.59)$$

or

$$\boxed{[\text{BWFN}]_{\phi=0} \approx \frac{2\lambda}{a}} \quad (10.60a)$$

Similarly,

$$\boxed{[\text{BWFN}]_{\phi=90^\circ} \approx \frac{2\lambda}{b}} \quad (10.60b)$$

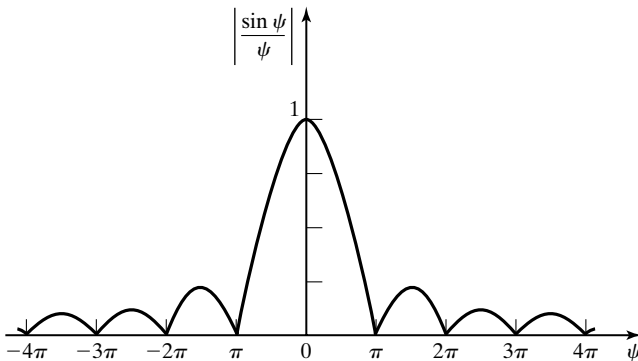


FIGURE 10.24

Variation of $|(\sin \psi)/\psi|$ with ψ , pertinent to the radiation pattern for the rectangular aperture antenna of Fig. 10.23.

Finally, we consider the determination of the directivity of the rectangular aperture antenna. To do this, it is convenient to use the basic definition that

$$D = \frac{[P_r]_{\max}}{[P_r]_{\text{av}}} = \frac{\langle P_r \rangle_{\max}}{\langle P_r \rangle_{\text{av}}} = \frac{4\pi r^2 \langle P_r \rangle_{\max}}{\langle P_{\text{rad}} \rangle} \quad (10.61)$$

instead of using (10.27), since P_{rad} , the power radiated from the antenna, being the same as that passing through the aperture, is much easier to compute from the aperture field distribution as compared to the evaluation of the integral in (10.27). Thus, in view of the uniform distribution of $\bar{\mathbf{E}}(x, y, 0) = E_0 \mathbf{a}_y$ in the aperture,

$$\langle P_{\text{rad}} \rangle = \frac{1}{2} \frac{E_0^2}{\eta_0} (ab) \quad (10.62)$$

and from (10.55),

$$\begin{aligned} \bar{E}_{\max} &= \frac{j\beta E_0 a b e^{-j\beta r}}{2\pi r} \\ \langle P_r \rangle_{\max} &= \frac{1}{2} \frac{|\bar{E}_{\max}|^2}{\eta_0} \\ &= \frac{\beta^2 E_0^2 a^2 b^2}{8\pi^2 r^2 \eta_0} \end{aligned} \quad (10.63)$$

Substituting (10.62) and (10.63) into (10.61), we obtain

$$D = \frac{\beta^2 ab}{\pi} = \frac{4\pi}{\lambda^2} (ab) \quad (10.64)$$

This result tells us that the directivity of the rectangular aperture antenna is $4\pi/\lambda^2$ times the physical aperture, ab . Although we have derived it here for the rectangular aperture, it is true for an aperture of any shape with uniform excitation.

K10.5. Aperture antenna; Far field; Rectangular aperture; Uniform excitation; BWFN.

D10.9. For the rectangular aperture antenna of Fig. 10.23, the BWFN in the $\phi = 0$ plane is 0.1 rad and the directivity is 800π . Find the following in degrees: **(a)** the BWFN in the $\phi = 90^\circ$ plane; **(b)** the half-power beamwidth (HPBW), that is, twice the value of θ for which the power density is one-half of the maximum power density in the $\phi = 0$ plane; and **(c)** the beamwidth between the first secondary maxima in the $\phi = 0$ plane.

Ans. **(a)** 11.46; **(b)** 2.54; **(c)** 8.19.

10.7 RECEIVING PROPERTIES

Reciprocity

Thus far, we have considered the radiating, or transmitting, properties of antennas. Fortunately, it is not necessary to repeat all the derivations for the discussion

of the receiving properties of antennas since reciprocity dictates that the receiving pattern of an antenna be the same as its transmitting pattern. To illustrate this in simple terms without going through the general proof of reciprocity, let us consider a Hertzian dipole situated at the origin and directed along the z -axis, as shown in Fig. 10.25. We know that the radiation pattern is then given by $\sin \theta$ and that the polarization of the radiated field is such that the electric field is in the plane of the dipole axis.

To investigate the receiving properties of the Hertzian dipole, we assume that it is situated in the radiation field of a second antenna so that the incoming waves are essentially uniform plane waves. Thus, let us consider a uniform plane wave with its electric field \mathbf{E} in the plane of the dipole and incident on the dipole at an angle θ with its axis, as shown in Fig. 10.25. Then the component of the incident electric field parallel to the dipole is $E \sin \theta$. Since the dipole is infinitesimal in length, the voltage induced in the dipole, which is the line integral of the electric-field intensity along the length of the dipole, is simply equal to $(E \sin \theta) dl$ or to $E dl \sin \theta$. This indicates that for a given amplitude of the incident wave field, the induced voltage in the dipole is proportional to $\sin \theta$. Furthermore, for an incident uniform plane wave having its electric field normal to the dipole axis, the voltage induced in the dipole is zero; that is, the dipole does not respond to polarization with electric field normal to the plane of its axis. These properties are reciprocal to the transmitting properties of the dipole. Since an arbitrary antenna can be decomposed into a series of Hertzian dipoles, it then follows that reciprocity holds for an arbitrary antenna. Thus, the receiving pattern of an antenna is the same as its transmitting pattern.

Let us consider the loop antenna, a common type of receiving antenna. A simple form of loop antenna consists of a circular loop of wire with a pair of terminals. We shall orient the circular loop antenna with its axis aligned with the z -axis, as shown in Fig. 10.26, and we shall assume that it is electrically short;

*Loop
antenna*

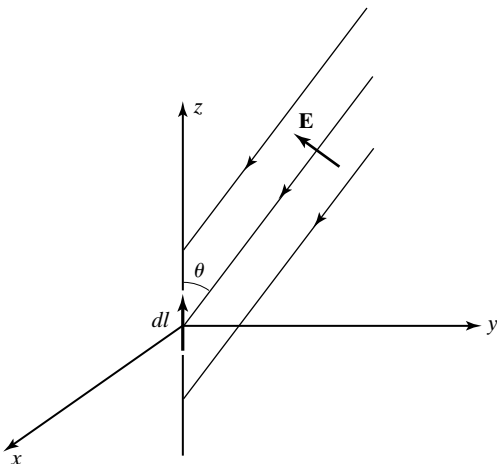


FIGURE 10.25

For investigating the receiving properties of a Hertzian dipole.

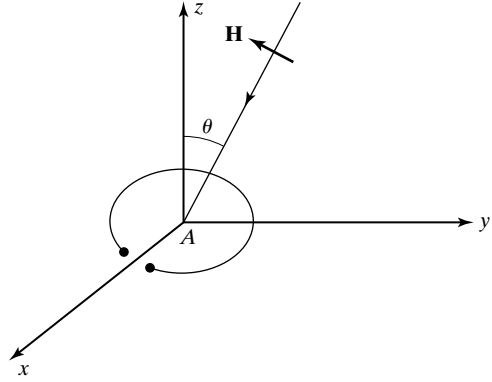


FIGURE 10.26
Circular loop antenna.

that is, its dimensions are small compared to the wavelength of the incident wave, so that the spatial variation of the field over the area of the loop is negligible. For a uniform plane wave incident on the loop, we can find the voltage induced in the loop, that is, the line integral of the electric-field intensity around the loop, by using Faraday's law. Thus, if \mathbf{H} is the magnetic-field intensity associated with the wave, the magnitude of the induced voltage is given by

$$\begin{aligned}
 |V| &= \left| -\frac{d}{dt} \int_{\text{area of the loop}} \mathbf{B} \cdot d\mathbf{S} \right| \\
 &= \left| -\mu \frac{d}{dt} \int_{\text{area of the loop}} \mathbf{H} \cdot dS \mathbf{a}_z \right| \\
 &= \mu A \left| \frac{\partial H_z}{\partial t} \right|
 \end{aligned} \tag{10.65}$$

where A is the area of the loop. Hence, the loop does not respond to a wave having its magnetic field entirely parallel to the plane of the loop, that is, normal to the axis of the loop.

For a wave having its magnetic field in the plane of the axis of the loop and incident on the loop at an angle θ with its axis, as shown in Fig. 10.26, $H_z = H \sin \theta$ and, hence, the induced voltage has a magnitude

$$|V| = \mu A \left| \frac{\partial H}{\partial t} \right| \sin \theta \tag{10.66}$$

Thus, the receiving pattern of the loop antenna is given by $\sin \theta$, the same as that of a Hertzian dipole aligned with the axis of the loop antenna. The loop antenna, however, responds best to polarization with the magnetic field in the plane of its axis, whereas the Hertzian dipole responds best to polarization with the electric field in the plane of its axis.

Example 10.6 Principle of radio source location using two loop antennas

The directional properties of a receiving antenna can be used to locate the source of an incident signal. To illustrate the principle, as already discussed in Section 2.3, let us consider two vertical loop antennas, numbered 1 and 2, situated on the x -axis at $x = 0$ m and $x = 200$ m, respectively. By rotating the loop antennas about the vertical (z -axis), it is found that no (or minimum) signal is induced in antenna 1 when it is in the xz -plane and in antenna 2 when it is in a plane making an angle of 5° with the axis, as shown by the top view in Fig. 10.27. Let us find the location of the source of the signal.

Since the receiving properties of a loop antenna are such that no signal is induced for a wave arriving along its axis, the source of the signal is located at the intersection of the axes of the two loops when they are oriented so as to receive no (or minimum) signal. From simple geometrical considerations, the source of the signal is therefore located on the y -axis at $y = 200/\tan 5^\circ$, or 2.286 km.

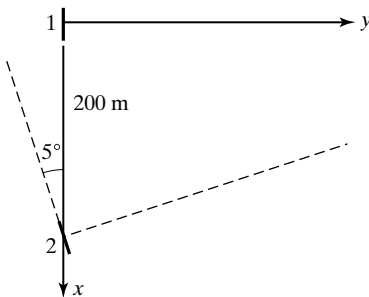


FIGURE 10.27

Top view of two loop antennas used to locate the source of an incident signal.

A useful parameter associated with the receiving properties of an antenna is the effective area, denoted A_e and defined as the ratio of the time-average power delivered to a matched load connected to the antenna to the time-average power density of the appropriately polarized incident wave at the antenna. The matched condition is achieved when the load impedance is equal to the complex conjugate of the antenna impedance.

Effective area

Let us consider the Hertzian dipole and derive the expression for its effective area. First, with reference to the equivalent circuit shown in Fig. 10.28, where \bar{V}_{oc} is the open-circuit voltage induced between the terminals of the antenna,

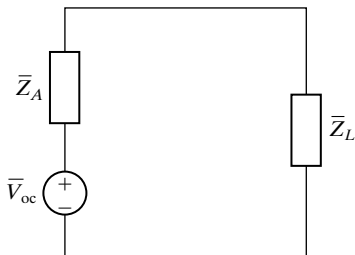


FIGURE 10.28

Equivalent circuit for a receiving antenna connected to a load.

$\bar{Z}_A = R_A + jX_A$ is the antenna impedance, and $\bar{Z}_L = \bar{Z}_A^*$ is the load impedance, we note that the time-average power delivered to the matched load is

$$P_R = \frac{1}{2} \left(\frac{|\bar{V}_{oc}|}{2R_A} \right)^2 R_A = \frac{|\bar{V}_{oc}|^2}{8R_A} \quad (10.67)$$

For a Hertzian dipole of length l , the open-circuit voltage is

$$\bar{V}_{oc} = \bar{E}l \quad (10.68)$$

where \bar{E} is the electric field of an incident wave linearly polarized parallel to the dipole axis. Substituting (10.68) into (10.67), we get

$$P_R = \frac{|\bar{E}|^2 l^2}{8R_A} \quad (10.69)$$

For a lossless dipole, $R_A = R_{rad} = 80\pi^2(l/\lambda)^2$, so that

$$P_R = \frac{|\bar{E}|^2 \lambda^2}{640\pi^2} \quad (10.70)$$

The time-average power density at the antenna is

$$\frac{|\bar{E}|^2}{2\eta_0} = \frac{|\bar{E}|^2}{240\pi} \quad (10.71)$$

Thus, the effective area is

$$A_e = \frac{|\bar{E}|^2 \lambda^2 / 640\pi^2}{|\bar{E}|^2 / 240\pi} = \frac{3\lambda^2}{8\pi} \quad (10.72)$$

or

$$\boxed{A_e = 0.1194\lambda^2} \quad (10.73)$$

In practice, R_A is greater than R_{rad} due to losses in the antenna, and the effective area is less than that given by (10.73). Rewriting (10.72) as

$$A_e = 1.5 \times \frac{\lambda^2}{4\pi}$$

and recalling that the directivity of the Hertzian dipole is 1.5, we observe that

$$\boxed{A_e = \frac{\lambda^2}{4\pi} D} \quad (10.74)$$

Although we have obtained this result for a Hertzian dipole, it can be shown that it holds for any antenna. It is of interest to note from (10.74) and (10.64) that the effective area of a rectangular aperture antenna for uniform field distribution in the aperture is equal to the physical aperture, which is to be expected.

We shall now derive the *Friis transmission formula*, an important equation in making communication link calculations. To do this, let us consider two antennas, one transmitting and the other receiving, separated by a distance d . Let us assume that the antennas are oriented and polarization matched so as to maximize the received signal. Then if P_T is the transmitter power radiated by the transmitting antenna, the power density at the receiving antenna is $(P_T/4\pi d^2) D_T$, where D_T is the directivity of the transmitting antenna. The power received by a matched load connected to the terminals of the receiving antenna is then given by

*Friis
transmission
formula*

$$P_R = \frac{P_T D_T}{4\pi d^2} A_{eR} \quad (10.75)$$

where A_{eR} is the effective area of the receiving antenna. Thus, the ratio of P_R to P_T is given by

$$\frac{P_R}{P_T} = \frac{D_T A_{eR}}{4\pi d^2} \quad (10.76)$$

Denoting A_{eT} to be the effective area of the transmitting antenna if it were receiving and using (10.74), we obtain

$$\boxed{\frac{P_R}{P_T} = \frac{A_{eT} A_{eR}}{\lambda^2 d^2}} \quad (10.77)$$

Equation (10.77) is the Friis transmission formula. It gives the maximum value of P_R/P_T for a given d and for a given pair of transmitting and receiving antennas. If the antennas are not oriented to receive the maximum signal, or if a polarization mismatch exists, or if the receiving antenna is not matched to its load, P_R/P_T would be less than that given by (10.77). Losses in the antennas would also decrease the value of P_R/P_T .

An alternative formula to (10.77) is obtained by substituting for A_{eR} in (10.76) in terms of the directivity D_R of the receiving antenna if it were used for transmitting. Thus, we obtain

$$\boxed{\frac{P_R}{P_T} = \frac{D_T D_R \lambda^2}{16\pi^2 d^2}} \quad (10.78)$$

K10.6. Receiving pattern; Reciprocity with transmitting pattern; Effective area; Communication link; Friis transmission formula.

D10.10. A communication link in free space uses two linear antennas of equal lengths L , oriented parallel to each other and normal to the line joining their centers. The antennas are separated by a distance $d = 1$ km. Find the maximum value of P_R/P_T for each of the following cases: **(a)** $L = 1$ m, $f = 10$ MHz; **(b)** $L = 1$ m, $f = 150$ MHz; and **(c)** $L = 2$ m, $f = 75$ MHz.

Ans. **(a)** 12.8×10^{-6} ; **(b)** 6.8×10^{-8} ; **(c)** 27.25×10^{-8} .

SUMMARY

In this chapter, we studied the principles of antennas. We first introduced the Hertzian dipole, which is an elemental wire antenna, and derived the electromagnetic field due to the Hertzian dipole by using the retarded magnetic vector potential. For a Hertzian dipole of length dl , oriented along the z -axis at the origin and carrying current

$$I(t) = I_0 \cos \omega t$$

we found the complete electromagnetic field to be given by

$$\begin{aligned} \mathbf{E} &= \frac{2I_0 dl \cos \theta}{4\pi\epsilon\omega} \left[\frac{\sin(\omega t - \beta r)}{r^3} + \frac{\beta \cos(\omega t - \beta r)}{r^2} \right] \mathbf{a}_r \\ &\quad + \frac{I_0 dl \sin \theta}{4\pi\epsilon\omega} \left[\frac{\sin(\omega t - \beta r)}{r^3} + \frac{\beta \cos(\omega t - \beta r)}{r^2} - \frac{\beta^2 \sin(\omega t - \beta r)}{r} \right] \mathbf{a}_\theta \\ \mathbf{H} &= \frac{I_0 dl \sin \theta}{4\pi} \left[\frac{\cos(\omega t - \beta r)}{r^2} - \frac{\beta \sin(\omega t - \beta r)}{r} \right] \mathbf{a}_\phi \end{aligned}$$

where $\beta = \omega\sqrt{\mu\epsilon}$ is the phase constant.

For $\beta r \gg 1$ or for $r \gg \lambda/2\pi$, the only important terms in the complete field expressions are the $1/r$ terms since the remaining terms are negligible compared to these terms. Thus, for $r \gg \lambda/2\pi$, the Hertzian dipole fields are given by

$$\begin{aligned} \mathbf{E} &= -\frac{\eta\beta I_0 dl \sin \theta}{4\pi r} \sin(\omega t - \beta r) \mathbf{a}_\theta \\ \mathbf{H} &= -\frac{\beta I_0 dl \sin \theta}{4\pi r} \sin(\omega t - \beta r) \mathbf{a}_\phi \end{aligned}$$

where $\eta = \sqrt{\mu/\epsilon}$ is the intrinsic impedance of the medium. These fields, known as the radiation fields, correspond to locally uniform plane waves radiating away from the dipole and, in fact, are the only components of the complete fields contributing to the time-average radiated power. We found the time-average power radiated by the Hertzian dipole to be given by

$$\langle P_{\text{rad}} \rangle = \frac{1}{2} I_0^2 \left[\frac{2\pi\eta}{3} \left(\frac{dl}{\lambda} \right)^2 \right]$$

and identified the quantity inside the brackets to be its radiation resistance. The radiation resistance, R_{rad} , of an antenna is the value of a fictitious resistor that will dissipate the same amount of time-average power as that radiated by the antenna when a current of the same peak amplitude as that in the antenna is passed through it. Thus, for the Hertzian dipole,

$$R_{\text{rad}} = \frac{2\pi\eta}{3} \left(\frac{dl}{\lambda} \right)^2$$

We then examined the directional characteristics of the radiation fields of the Hertzian dipole as indicated by the factor $\sin \theta$ in the field expressions and hence by the factor $\sin^2 \theta$ for the power density. We discussed the radiation patterns and introduced the concept of the directivity of an antenna. The directivity, D , of an antenna is defined as the ratio of the maximum power density radiated by the antenna to the average power density. For the Hertzian dipole,

$$D = 1.5$$

For the general case of a power density pattern $f(\theta, \phi)$, the directivity is given by

$$D = 4\pi \frac{[f(\theta, \phi)]_{\max}}{\int_{\theta=0}^{\pi} \int_{\phi=0}^{2\pi} f(\theta, \phi) \sin \theta \, d\theta \, d\phi}$$

As an illustration of obtaining the radiation fields due to a wire antenna of arbitrary length and arbitrary current distribution by representing it as a series of Hertzian dipoles and using superposition, we considered the example of a center-fed half-wave dipole of length $L (= \lambda/2)$, oriented along the z -axis with its center at the origin and having the current distribution given by

$$I(z) = I_0 \cos \frac{\pi z}{L} \cos \omega t \quad \text{for} \quad -L/2 < z < L/2$$

and found that the radiation fields are

$$\begin{aligned} \mathbf{E} &= -\frac{\eta I_0}{2\pi r} \frac{\cos[(\pi/2) \cos \theta]}{\sin \theta} \sin\left(\omega t - \frac{\pi}{L} r\right) \mathbf{a}_\theta \\ \mathbf{H} &= -\frac{I_0}{2\pi r} \frac{\cos[(\pi/2) \cos \theta]}{\sin \theta} \sin\left(\omega t - \frac{\pi}{L} r\right) \mathbf{a}_\phi \end{aligned}$$

From these, we sketched the radiation patterns and computed the radiation resistance and the directivity of the half-wave dipole to be

$$\begin{aligned} R_{\text{rad}} &= 73 \, \Omega \quad \text{for free space} \\ D &= 1.642 \end{aligned}$$

We then extended the computation of these quantities to the case of a center-fed linear antenna of length equal to an arbitrary number of wavelengths.

We discussed antenna arrays and introduced the technique of obtaining the resultant radiation pattern of an array by multiplication of the unit and the group patterns. For an array of two antennas having the spacing d and fed with currents of equal amplitude but differing in phase by α , we found the group pattern for the fields to be $|\cos[(\beta d \cos \psi + \alpha)/2]|$, where ψ is the angle measured from the axis of the array, and we investigated the group patterns for several pairs of values of d and α . For example, for $d = \lambda/2$ and $\alpha = 0$, the pattern

corresponds to maximum radiation broadside to the axis of the array, whereas for $d = \lambda/2$ and $\alpha = \pi$, the pattern corresponds to maximum radiation endfire to the axis of the array. We generalized the treatment to a uniform linear array of n antennas and briefly discussed the principle of a broadband array.

To take into account the effect of ground on antennas, we introduced the concept of an image antenna in a perfect conductor and discussed the application of the array techniques in conjunction with the actual and the image antennas to obtain the radiation pattern of the actual antenna in the presence of the ground. As another example of the image-antenna concept, we considered the corner reflector.

Next we discussed the far-field determination for an aperture antenna by recalling that it is equivalent to setting up the problem to solve for Fraunhofer diffraction from the aperture, which consists of using the plane wave approximation. By considering the example of a rectangular aperture with uniform field distribution in it, we illustrated the solution and studied the resulting radiation pattern and its characteristics.

Finally, we discussed receiving properties of antennas. In particular, (1) we discussed the reciprocity between the receiving and radiating properties of an antenna by considering the simple case of a Hertzian dipole, (2) we considered the loop antenna and illustrated the application of its directional properties for locating the source of a radio signal, and (3) we introduced the effective area concept and derived the Friis transmission formula.

REVIEW QUESTIONS

- Q10.1.** What is a Hertzian dipole? Discuss the time variations of the current and charges associated with the Hertzian dipole.
- Q10.2.** Discuss the analogy between the magnetic vector potential due to an infinitesimal current element and the electric scalar potential due to a point charge.
- Q10.3.** To what does the word *retarded* in the terminology *retarded magnetic vector potential* refer? Explain.
- Q10.4.** Outline the derivation of the electromagnetic field due to the Hertzian dipole.
- Q10.5.** Discuss the characteristics of the electromagnetic field due to the Hertzian dipole.
- Q10.6.** What are radiation fields? Why are they important? Discuss their characteristics.
- Q10.7.** Define the radiation resistance of an antenna.
- Q10.8.** Why is the expression for the radiation resistance of a Hertzian dipole not valid for a linear antenna of any length?
- Q10.9.** What is a radiation pattern?
- Q10.10.** Discuss the radiation pattern for the power density due to the Hertzian dipole.
- Q10.11.** Define the directivity of an antenna. What is the directivity of a Hertzian dipole?
- Q10.12.** How do you find the radiation fields due to an antenna of arbitrary length and arbitrary current distribution?
- Q10.13.** Discuss the evolution of the half-wave dipole from an open-circuited transmission line.
- Q10.14.** Justify the approximations involved in evaluating the integrals in the determination of the radiation fields due to the half-wave dipole.

- Q10.15.** What are the values of the radiation resistance and the directivity for a half-wave dipole?
- Q10.16.** What is an antenna array?
- Q10.17.** Justify the approximations involved in the determination of the resultant field of an array of two antennas.
- Q10.18.** What is an array factor? Provide a physical explanation for the array factor.
- Q10.19.** Discuss the concept of unit and group patterns and their multiplication to obtain the resultant pattern of an array.
- Q10.20.** Distinguish between broadside and endfire radiation patterns.
- Q10.21.** Discuss the principle of a phased array.
- Q10.22.** Discuss the principle of a broadband array using as an example the log-periodic dipole array.
- Q10.23.** Discuss the concept of an image antenna to find the field of an antenna in the vicinity of a perfect conductor.
- Q10.24.** What determines the sense of the current flow in an image antenna relative to that in the actual antenna?
- Q10.25.** How does the concept of an image antenna simplify the determination of the radiation pattern of an antenna above a perfect conductor surface?
- Q10.26.** Discuss the application of the image-antenna concept to the 90° corner reflector.
- Q10.27.** Explain the distinguishing feature pertinent to the computation of radiation from an aperture antenna.
- Q10.28.** Give examples of aperture antennas.
- Q10.29.** Discuss the determination of the far field for an aperture antenna.
- Q10.30.** Describe the radiation pattern for the far field of a rectangular aperture antenna with uniform field distribution in the aperture and discuss its characteristics.
- Q10.31.** Discuss the reciprocity associated with the transmitting and receiving properties of an antenna. Can you think of a situation in which reciprocity does not hold?
- Q10.32.** What is the receiving pattern of a loop antenna? How should you orient a loop antenna to receive **(a)** a maximum signal and **(b)** a minimum signal?
- Q10.33.** Discuss the application of the directional receiving properties of a loop antenna in the location of the source of a radio signal.
- Q10.34.** How is the effective area of a receiving antenna defined?
- Q10.35.** Outline the derivation of the expression for the effective area of a Hertzian dipole.
- Q10.36.** Discuss the derivation of the Friis transmission formula.

PROBLEMS

Section 10.1

- P10.1. Satisfaction of Maxwell's curl equation for \mathbf{E} by Hertzian dipole fields.** Show that (10.9) and (10.10) satisfy the Maxwell's curl equation for \mathbf{E} .
- P10.2. Some characteristics of the Poynting vector for Hertzian dipole fields.** For the electromagnetic field due to the Hertzian dipole, show that **(a)** the time-average value of the θ -component of the Poynting vector is zero and **(b)** the contribution to the time-average value of the r -component of the Poynting vector is completely from the terms involving $1/r$.

- P10.3. Nonsatisfaction of Maxwell's curl equations by Hertzian dipole quasistatic fields.** Show that the field expressions obtained by replacing ωt in (10.11) and (10.12) by $(\omega t - \beta r)$ do not satisfy Maxwell's curl equations.
- P10.4. RMS values of Hertzian dipole field components for current of two frequencies.** A Hertzian dipole of length 1 m situated at the origin and oriented along the positive z -direction carries the current $10 \cos 2\pi \times 10^6 t \cos 6\pi \times 10^6 t$ A. Find the root-mean-square values of E_r , E_θ , and H_ϕ at the point $(10, \pi/3, 0)$. Assume free space for the medium.

Section 10.2

- P10.5. Nonsatisfaction of Maxwell's curl equations by the radiation fields of a Hertzian dipole.** Show that the radiation fields given by (10.17a) and (10.17b) do not by themselves satisfy simultaneously the Maxwell's curl equations.
- P10.6. Transition from near field to radiation field for E_θ of a Hertzian dipole.** Find the value of r at which the amplitude of the radiation field in the θ -component of \mathbf{E} in (10.10) is equal to the resultant amplitude of the remaining two terms.
- P10.7. Computation of Hertzian dipole current for producing a given electric field.** Find the amplitude I_0 of the current with which a Hertzian dipole of length 0.5 m has to be excited at a frequency of 10 MHz to produce an electric-field intensity of amplitude 1 mV/m at a distance of 1 km broadside to the dipole, in free space. What is the time-average power radiated for the computed value of I_0 ?
- P10.8. Computation of directivity of an antenna for a given power density radiation pattern.** The power density pattern for an antenna located at the origin is given by

$$f(\theta, \phi) = \begin{cases} \csc^2 \theta & \text{for } \pi/6 \leq \theta \leq \pi/2 \\ 0 & \text{otherwise} \end{cases}$$

Find the directivity of the antenna.

- P10.9. Current ratio for two antennas with equal maximum radiated power densities.** Find the ratio of the currents in two antennas having directivities D_1 and D_2 and radiation resistances $R_{\text{rad}1}$ and $R_{\text{rad}2}$ for which the maximum time-average radiated power densities are equal.
- P10.10. Computation of time-average power radiated by a Hertzian dipole.** For the Hertzian dipole of Problem P10.4, calculate the time-average power radiated by the dipole.

Section 10.3

- P10.11. Magnetic vector potential and radiation fields for a half-wave dipole.** For the half-wave dipole of Section 10.3, find the magnetic vector potential for the radiation fields and show that the radiation fields obtained from it are the same as those given by (10.31a) and (10.31b).
- P10.12. Computation of a linear dipole current for producing a given electric field.** Find the maximum amplitude I_0 of the current with which a linear dipole of length 15 m has to be excited at a frequency of 10 MHz in order to produce an electric-field intensity of amplitude 1 mV/m at a distance of 1 km broadside to the dipole, in free space. What is the time-average power radiated for the computed value of I_0 ?

- P10.13. Computation of a linear dipole current for producing a given electric field.** Repeat Problem P10.12 for a linear dipole of length 15 m at a frequency of 50 MHz.
- P10.14. Derivation of radiation fields and characteristics for a short dipole.** A short dipole is a center-fed straight-wire antenna having a length small compared to a wavelength. The amplitude of the current distribution can then be approximated as decreasing linearly from a maximum at the center to zero at the ends. Thus, for a short dipole of length L lying along the z -axis between $z = -L/2$ and $z = L/2$, the current distribution is given by

$$I(z) = \begin{cases} I_0 \left(1 + \frac{2z}{L}\right) \cos \omega t & \text{for } -L/2 < z < 0 \\ I_0 \left(1 - \frac{2z}{L}\right) \cos \omega t & \text{for } 0 < z < L/2 \end{cases}$$

- (a) Obtain the radiation fields of the short dipole. (b) Find the radiation resistance and the directivity of the short dipole.
- P10.15. Derivation of radiation fields for a circular loop antenna.** Consider a circular loop antenna of radius a such that the circumference is small compared to the wavelength. Assume the loop antenna to be in the xy -plane with its center at the origin and the loop current to be $I = I_0 \cos \omega t$ in the sense of increasing ϕ . Show that for obtaining the radiation fields, the magnetic vector potential due to the loop antenna is given by

$$\mathbf{A} = \frac{\mu_0 I_0 \pi a^2 \beta \sin \theta}{4\pi r} \sin(\omega t - \beta r) \mathbf{a}_\phi$$

where $\beta = \omega/v_p$. Then show that the radiation fields are

$$\begin{aligned} \mathbf{E} &= \frac{\eta I_0 \pi a^2 \beta^2 \sin \theta}{4\pi r} \cos(\omega t - \beta r) \mathbf{a}_\phi \\ \mathbf{H} &= -\frac{I_0 \pi a^2 \beta^2 \sin \theta}{4\pi r} \cos(\omega t - \beta r) \mathbf{a}_\theta \end{aligned}$$

- P10.16. Radiation resistance and directivity of a circular loop antenna.** Find the radiation resistance and the directivity of the circular loop antenna of Problem P10.15. Compare the dependence of the radiation resistance on the electrical size (circumference/wavelength) to the dependence of the radiation resistance of the Hertzian dipole on its electrical size (length/wavelength).

Section 10.4

- P10.17. Group patterns for several cases of an array of two antennas.** For the array of two antennas of Example 10.3, find and sketch the group pattern for each of the following cases: (a) $d = \lambda$, $\alpha = \pi/2$; and (b) $d = 2\lambda$, $\alpha = 0$.
- P10.18. Resultant pattern for an array of two Hertzian dipoles in the plane of the array.** For the array of two Hertzian dipoles of Fig. 10.11, find and sketch the resultant pattern in the xz -plane for each of the following cases: (a) $d = \lambda/2$, $\alpha = \pi$; and (b) $d = \lambda/4$, $\alpha = -\pi/2$.

- P10.19. Group pattern for a linear binomial array.** For a linear binomial array of n antennas, the amplitudes of the currents in the elements are proportional to the coefficients in the polynomial $(1 + x)^{n-1}$. Show that the group pattern is $|\cos[(\beta d \cos \psi + \alpha)/2]|^{n-1}$, where d is the spacing between the elements and α is the progressive phase shift.
- P10.20. Beam width between first nulls for the radiation pattern of a large uniform linear array.** For the uniform linear array of n isotropic antennas of Fig. 10.15, assume that $\alpha = 0$ so that the group pattern is a broadside pattern. Show that for large n and for $nd \gg \lambda$, the beam width between the first nulls (BWFN), that is, the angular spacing between the nulls on either side of the main lobe of the group pattern, is approximately equal to $2\lambda/L$, where L is the length of the array.
- P10.21. Synthesis of an array for a given group pattern using pattern multiplication technique.** Use the pattern multiplication technique in reverse to synthesize an array of isotropic elements for the group pattern

$$\cos^2\left(\frac{\pi}{2} \cos \psi\right) \left| \sin\left(\frac{\pi}{2} \cos \psi\right) \right|$$

- P10.22. Synthesis of an array for a given group pattern using pattern multiplication technique.** Repeat Problem P10.21 for the group pattern

$$\frac{\cos^2(6\pi \cos \psi)}{9 \cos^2(2\pi \cos \psi)}$$

Section 10.5.

- P10.23. Radiation patterns for a horizontal half-wave dipole quarter wavelength above ground.** For a horizontal half-wave dipole at a height $\lambda/4$ above a plane, perfect conductor surface, find and sketch the radiation pattern in (a) the vertical plane perpendicular to the axis of the antenna and (b) the vertical plane containing the axis of the antenna.
- P10.24. Radiation characteristics for a vertical quarter-wavelength antenna above ground.** For a vertical antenna of length $\lambda/4$ above a plane, perfect conductor surface, find (a) the radiation pattern in the vertical plane and (b) the directivity.
- P10.25. A Hertzian dipole in the presence of a 90° corner reflector.** A Hertzian dipole is situated parallel to one side and perpendicular to the other side of a 90° corner reflector, as shown in Fig. 10.29. Find the expression for the radiation pattern in the plane of the paper as a function of the angle θ and the distances d_1 and d_2 .

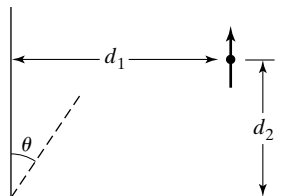


FIGURE 10.29
For Problem P10.25.

- P10.26. A quarter-wavelength monopole in the presence of a 90° corner reflector.** A $\lambda/4$ monopole is situated parallel to one side and perpendicular to the other side of a 90° corner reflector, as shown in Fig. 10.30. Find the radiation pattern in the plane of the paper as a function of the angle θ .

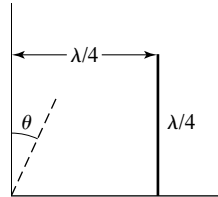


FIGURE 10.30

For Problem P10.26

- P10.27. A Hertzian dipole in the presence of a 60° corner reflector.** A corner reflector is made up of two semi-infinite plane, perfect conductors at an angle of 60°, as shown by the cross-sectional view in Fig. 10.31. A Hertzian dipole is situated parallel to the conductors at a distance of $k\lambda$ from the corner along the bisector of the two conductors. Find the ratio of the radiation field at a point broadside to the dipole and along the bisector of the conductors to the radiation field at the same point in the absence of the corner reflector, for the following values of k : (a) $\frac{1}{4}$; (b) $\frac{1}{2}$; and (c) 1.

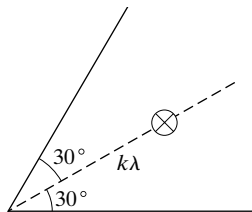


FIGURE 10.31

For Problem P10.27.

Section 10.6

- P10.28. Far field for a rectangular aperture antenna with nonuniform field distribution.** For the rectangular aperture antenna of Example 10.5, assume that the field distribution in the aperture is nonuniform as given by

$$\bar{\mathbf{E}}(x, y, 0) = E_0 \cos \frac{\pi x}{a} \mathbf{a}_y \quad \text{for} \quad -a/2 < x < a/2, -b/2 < y < b/2$$

Obtain the expression for the far field and hence the expressions for the following: (a) BWFN in the $\phi = 0$ plane; (b) BWFN in the $\phi = 90^\circ$ plane; (c) HPBW in the $\phi = 0$ plane; and (d) the directivity.

- P10.29. Far field for a rectangular aperture antenna with nonuniform field distribution.** Repeat Problem P10.28 for

$$\bar{\mathbf{E}}(x, y, 0) = E_0 \cos^2 \frac{\pi x}{a} \mathbf{a}_y \quad \text{for} \quad -a/2 < x < a/2, -b/2 < y < b/2$$

- P10.30. Far field radiation pattern for a circular aperture with uniform field distribution.** Consider a circular aperture of radius a in the xy -plane and centered at the origin. For uniform field distribution $\mathbf{E} = E_0 \mathbf{a}_x$ in the aperture, show that the far-field radiation pattern is in accordance with $J_1(\beta a \sin \theta)/(\beta a \sin \theta)$. Further, given that the first nonzero root of $J_1(x) = 0$ is 3.83, show that in any constant- ϕ -plane, the BWFN is approximately equal to $1.22\lambda/a$.

$$\left[\text{Note: } \frac{1}{2\pi} \int_0^{2\pi} e^{ix \cos \alpha} d\alpha = J_0(x) \text{ and } \int x J_0(x) dx = x J_1(x) \right]$$

- P10.31. Radiation pattern for a large uniform linear array of isotropic antennas.** Consider the uniform linear array of n isotropic antennas of Fig. 10.15 for the case of $\alpha = 0$ so that the group pattern is a broadside pattern. Show that for large n and for $nd \gg \lambda$, the radiation pattern is the same as that in one of the coordinate planes ($\phi = 0$ or $\phi = 90^\circ$) for the rectangular aperture antenna with uniform field distribution of Example 10.5, and hence the BWFN is approximately equal to $2\lambda/L$, where L is the length of the array.

Section 10.7

- P10.32. Application of a turnstile antenna for responding to clockwise circular polarization.** An arrangement of two identical Hertzian dipoles situated at the origin and oriented along the x - and y -axes, known as the turnstile antenna, is used for receiving circularly polarized signals arriving along the z -axis. Determine how you would combine the voltages induced in the two dipoles so that the turnstile antenna is responsive to circular polarization rotating in the clockwise sense as viewed by the antenna, but not to that of the counterclockwise sense of rotation.
- P10.33. Ambiguity in the application of an interferometer for angle-of-arrival measurement.** A uniform plane wave is incident on an interferometer consisting of an array of two identical antennas with spacing $d = 3\lambda$ at an angle $\psi = 50^\circ$ to the axis of the array, producing a phase difference $\Delta\phi$ between the voltages induced in the two antennas. Find all possible values of $0^\circ < \psi < 180^\circ$ that result in a phase difference equal to $\Delta\phi \pm 2n\pi$, where n is an integer, between the two induced voltages.
- P10.34. A communication link involving a half-wave dipole and a small loop antenna.** A communication link at a frequency of 30 MHz uses a half-wave dipole for the transmitting antenna and a small loop for the receiving antenna, involving a distance of 100 km. The antennas are oriented so as to receive maximum signal and the receiving antenna is matched to its load. If the received time-average power is to be $1 \mu\text{W}$, find the minimum required value of the maximum amplitude I_0 of the current with which the transmitting antenna has to be excited. Assume the antennas to be lossless.

REVIEW PROBLEMS

- R10.1. Locus of circular polarization for the radiation field of a turnstile antenna.** Two identical current elements are located at the origin, one directed along the positive x -axis and the other directed along the positive z -axis. They carry currents equal in amplitude and 90° out of phase. Find the expression for the locus of all

points at which the polarization of the field is circular on the surface of a sphere of radius r , where $\beta r \gg 1$.

R10.2. Three-dimensional power density pattern of an array of two Hertzian dipoles.

For the array of two Hertzian dipoles in Fig. 10.11, assume that $d \ll \lambda$ and $\alpha = \pi$. Obtain an approximate expression for the three-dimensional power density pattern $f(\theta, \phi)$ and find the directivity and the radiation resistance.

R10.3. Radiation pattern of a center-fed antenna an odd multiple of half-wavelengths long.

Show that the radiation pattern for a center-fed linear antenna of length equal to an odd-integer number of half-wavelengths, n , obtained by setting $k = n/2$ in (10.41), agrees with the one obtained by considering the antenna as an array of n half-wave dipoles of currents of equal amplitudes and appropriate progressive phase shift.

R10.4. Synthesis of an array for a given group pattern using pattern multiplication technique.

Synthesize an array of isotropic elements for the group pattern

$$\frac{\sin(2\pi \cos \psi)}{\sin[(\pi/2) \cos \psi]} \cos^2\left(\frac{\pi}{2} \cos \psi\right)$$

R10.5. A Hertzian dipole in the presence of a 90° corner reflector. A Hertzian dipole is situated at a distance d from the corner along the bisector of the two conductors of a 90° corner reflector and oriented normal to the bisector in the cross-sectional plane, as shown in Fig. 10.32. Obtain the expression for the radiation pattern in the cross-sectional plane, as a function of the angle θ .

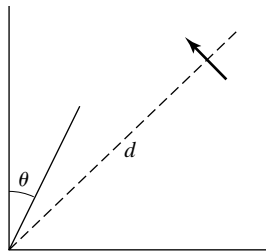


FIGURE 10.32

For Problem R10.5.

R10.6. Radiation pattern for a large uniform linear array of isotropic antennas.

Consider the uniform linear array of n isotropic antennas of Fig. 10.15 for the case of $\alpha = -\beta d$, so that the group pattern is an endfire pattern. Show that for large n and for $nd \gg \lambda$, the BWFN is approximately equal to $\sqrt{8\lambda/L}$.